Resonant Franz-Keldysh exciton effect in the narrow biased quantum wire subject to a strong magnetic field

B. S. Monozon
Department of Physics, Marine Technical University, 3 Lotsmanskaya Strasse, 190008 St. Petersburg, Russia

P. Schmelcher
Theoretische Chemie, Institut für Physikalische Chemie der Universität Heidelberg, INF 229, 69120 Heidelberg, Germany

(Received 16 July 2008; revised manuscript received 6 February 2009; published 20 April 2009)

We present an analytical investigation of quasi-one-dimensional excitons in thin uniform (single) and double nanoscaled cylindrical quantum wires (UQWR and DQWR) surrounded by a barrier of infinite height and exposed to external electric and strong magnetic fields. The DQWR is formed by inserting an impenetrable longitudinal barrier in a single-quantum wire. Both external fields are directed parallel to the quantum wire (QWR) axis. The radius of the QWRs and the magnetic length are taken to be much less than the exciton Bohr radius. For the dependencies of the positions and widths of the complex quasidiscrete energy levels of the indirect exciton in the DQWR, in which the carriers are separated by the insertion on the confinement, electric field strength and width of the interwire barrier are derived. The confinement (insertion) leads to an increase (decrease) of the exciton binding energy. The impact of the electric field ionization of the exciton is less pronounced for strongly confined and weakly separated carriers. The coefficient of the exciton absorption in the UQWR as a function of the confinement and electric field is calculated in an explicit form. The effect of the confinement and electric field on the exciton peak closely resembles that on the quasidiscrete level of the indirect exciton in the DQWR. Electron-hole attraction increases remarkably the optical Franz-Keldysh electroabsorption in the frequency region below the edge and distant from the exciton peaks. The coefficient of absorption reflecting the electric field ionization and autoionization caused by the coupling between the discrete and continuous exciton states adjacent to the different size-quantized or Landau levels is obtained analytically. A comparison of our analytical results with numerical data is performed. Estimates of the expected experimental values for the parameters of GaAs/GaAlAs QWR show that the autoionized exciton magnetostates in thin biased QWRs are sufficiently stable to be observed.

DOI: 10.1103/PhysRevB.79.165314 PACS number(s): 73.63.Nm, 71.35.−y, 73.21.Hb

I. INTRODUCTION

At the present time the rapid advance in material growth technology such as electron-beam lithography and etching, growth on nonplanar and masked substrates, or molecular-beam epitaxy, leads to a renewed interest in the theoretical and experimental studies of semiconductor quantum wires (QWRs) (see Refs. 1–3, and references therein). The reason for this is that QWRs of high quality and well controlled parameters allow for unique properties of the one-dimensional (1D) electron and hole states. A study of the 1D structures is important on account of two aspects: (i) considerable interest in fundamental properties associated with the inverse square-root divergence of the energy density of the 1D states at the band gap E_g, manifesting itself in interband optical effects, and (ii) a wide range of potential applications, e.g., nanolasers, 1D wave guides, resonant tunneling diodes, thermoelectric systems,[4] metal complexes,[5] and porous silicon QWRs.[6]

Along with the uniform QWRs (UQWRs) the nonuniform wire structures attract much attention. Recently a theory of optical absorption in a quantum dot superlattice embedded in a QWR has been developed.[4] Gradećak *et al.*[7] demonstrated that *n*-GaN/InGaN/*p*-GaN radial wire heterostructures can be prepared and configured as light-emitting diodes. Efficient photoluminescence has been observed in InP/InAsP/InP structures formed by the InP QWR with embedded InAsP insertion.[8] Electronic properties of the single- and double-barrier InAs/InP wire structures were studied experimentally[9] and theoretically[10] in terms of the basic elements of the transport and photonic devices. Here we treat the single-barrier structure formed by two coaxial QWRs separated by impenetrable insertion as the double QWR (DQWR).

The external longitudinal uniform electric field F modifies the spectrum of the interband fundamental optical absorption [Franz-Keldysh (F-K) effect].[11–14] At the edge of spectrum $\hbar\omega=E_g$ the square-root singularity is replaced by a finite maximum. An electric field induces a nonvanishing absorption below the edge $\hbar\omega<E_g$ as well as oscillations above the edge $\hbar\omega>E_g$. Note that the F-K effect is most pronounced for a 1D QWR compared to two-dimensional (2D) quantum wells or to the three-dimensional (3D) bulk material. This is because in the QWR there are no degrees of freedom unaffected by the electric field while in the 2D structures or in bulk material one or two degrees of freedom, respectively, remain untouched.

Excitons formed by interacting electrons and holes change drastically the optical electroabsorption in QWRs.[2,3,15,16] Rydberg series of exciton peaks arise below the edge and tend to the finite absorption at the edge while above the edge the exciton effect suppresses the F-K optical absorption.

In the presence of a longitudinal dc electric field F, the exciton peaks become wider and less in intensity because of

the ionization of the bound exciton states. Under the condition $F>F_0$, where F_0 is the critical electric field determined by the exciton binding energy E_b and the exciton Bohr radius a_0,[16] the exciton states become ionizing and too wide to be accessible in an experimental study. This is why thin QWRs (nanowires) of radius R, being much smaller than the exciton Bohr radius a_0 ($R \ll a_0$) are of special interest. In units of the exciton Rydberg constant $\mathrm{Ry}^{(\mathrm{ex})}$ the binding energy of the exciton in bulk material is $E_b^{3\mathrm{D}}=1\mathrm{Ry}^{(\mathrm{ex})}$ and binding energy of the 2D exciton in quantum well is $E_b^{2\mathrm{D}}=4\mathrm{Ry}^{(\mathrm{ex})}$; the binding energy of the 1D exciton in the QWR, $E_b^{1\mathrm{D}} \simeq \mathrm{Ry}^{(\mathrm{ex})} \ln^2(R/a_0)$ $[a_0/R \gg 1, \ln(a_0/R) \gg 1]$, in principle, can be made significantly greater than those in the 2D and 3D structures. This in turn leads to an increase in the critical electric field F_0 and stability of the exciton with respect to ionization. The critical electric fields $F_0^{(\mathrm{qwr})}$, estimated from the data of Ref. 17 for the GaAs QWR of radius $R=4.2$ nm and for the bulk GaAs crystal $F_0^{(\mathrm{bulk})}$, obey the relationship $F_0^{(\mathrm{qwr})} \simeq 13.5 F_0^{(\mathrm{bulk})}$. Note that nanowires of radius $R=3.6$ and 4.2 nm were recently considered in Refs. 2 and 4, respectively, while the exciton Bohr radius in GaAs material is about $a_0=14$ nm.[16] Thus exciton effects in QWR become more pronounced and play an important role in the optical absorption close to the edge $\hbar\omega=E_g$. In the case $R>a_0$ the quasi-1D character of the exciton states can be ensured by a strong longitudinal magnetic field B providing the magnetic length $a_B=(\hbar/eB)^{1/2}$ to be much less than the exciton Bohr radius a_0 ($a_B \ll a_0$). In this case the exciton binding energy $E_b^{1\mathrm{D}}$ can be estimated using the above-given expression while replacing R by a_B. Detailed studies of magnetoexcitons originated in Refs. 17 and 18, and are followed by Refs. 1, 3, and 19–21.

Besides the direct excitons in the uniform low-dimensional structures, the indirect excitons composed of the spatially separated electrons and holes in nonuniform systems are under study. In particular the superfluidity of the indirect excitons in the quantum well[22] and quantum wire[23] structures was predicted (see Refs. 22 and 23, and references therein). The liquid phase is realized because the indirect exciton lifetime considerably exceeds the thermalization time on account of the small overlap of the spatially separated electron and hole states. The spatially indirect excitons and their liquid phase manifest themselves experimentally in the spectra of the photoluminescence of double quantum nanostructures.[24] Lozovik and Ruvinskii[22] pointed out that the electric field directed perpendicular to the heterolayers separating the carriers leads to an increase in effective electron-hole distance and hence to a decrease in the recombination rate. However, the electric field transforms the bound exciton into unbound electron-hole pair because of the ionization process. Thus, the effect of the electric field on the indirect excitons is of interest. Here we point out that in the present paper the indirect exciton is formed by the electron and hole in the coaxial quantum wires while in Ref. 23 electron and hole move in two parallel coupled quantum wires. In contrast to the coaxial wires, the coupled wire confinement, providing the indirect character of the exciton, acts perpendicular to the axis of the structure.

Under the condition $r_0 \ll a_0$ $[r_0=\min(R,a_B)]$ the total exciton energy consists of the sequence of the Rydberg energy series of the n states, $n=0,1,2,\ldots$, adjacent to the low side to the size-quantized ($R<a_B$) or Landau ($R>a_B$) levels $E_{\perp N}$, $N=0,1,2,\ldots$. All series except one, the energetically lowest $N=0$, are superimposed on the N subbands of the continuous quasi-Coulomb spectra emanating from the lower levels $E_{\perp N}$. Thus only the ground exciton series $N=0$ is strictly discrete while others ($N>0$) are quasidiscrete (i.e., Fano resonances[25]) because of the interlevel (intersubband) coupling between the nth discrete and continuum states of the same energy. The energy-level density corresponding to the excited series $N>0$ consists of peaks of finite width $\Gamma_{Nn}^{\perp}$ determining the autoionization rate and lifetime of the nth resonant state. In the presence of the electric field F the exciton states of the excited Rydberg series $N>0$ have two channels of ionization: the autoionization channel, caused by the intersubband coupling, and the electric field-ionization channel, associated with the below barrier tunneling, and providing the width Γ_{Nn}^{F} and field-ionization rate of the bound Coulomb states.[26] For the n states of the ground exciton series $N=0$ only one channel is opened, namely, the ionization by the electric field F. Clearly nanowires subjected to longitudinal electric and strong magnetic fields are unique structures in which an interplay between the exciton ionization rates related to $\Gamma_{Nn}^{\perp}$ and Γ_{Nn}^{F} occurs. The finite lifetime of the quasidiscrete exciton states is essential for an experimental study of the excitons in the nanowires exposed to electric fields.

Let us comment on the problem under discussion. First, the existing theoretical approaches are mostly based on numerical solutions (solving the semiconductor Bloch equations,[2,16] expansion in a basis set,[15] finite difference scheme,[3] and Poisson-Schrödinger calculations[10]) including variational methods[1,17–20] requiring a substantial computational efforts. Bednarek *et al.*[27] calculated the binding energy of the quasi-1D exciton in a QWR using 100 variational parameters. In parallel with this a detailed study of the evolution of the exciton spectrum as a function of the radius of the QWR, and strengths of the magnetic and electric fields remains unavailable. Although numerical approaches are indispensable for a detailed understanding and comparison with experimental data, it is at the same time instructive and complementary to develop and apply analytical methods which will be activated in the present work. Analytical approaches provide the possibility to follow the evolution of the exciton spectrum as a function of the radius of the QWR, and the electric and magnetic fields strengths. Note that strong exciton effect on the F-K electroabsorption in the spectral region off the exciton peaks in bulk material has been predicted analytically.[28,29] To our knowledge analytical methods providing the explicit dependencies are not widely available in the literature. Second, the absolute majority of papers employed the single-subband (SS) approximation, in which the coupling between the discrete and continuous exciton states was not taken into account.[2–4,15] A double-subband (DS) approximation describing the coupling between two pairs electron and heavy-hole subbands has been used in Ref. 16. However, the contribution of the autoionization to the presented numerical results was not clearly identified. Third, only few papers relate to the effects of electric and transverse magnetic fields on the exciton states in the

QWR. Benner and Haug[30] solving Poisson's and Schrödinger's equations consider separately the quantum confined Stark effect and magnetoabsorption in the QWR. Madureira *et al.*[31] calculated the magnetoexciton electroabsorption in T-shaped QWRs using the semiconductor Bloch equation. Again to our knowledge the combined effect of both longitudinal magnetic and electric fields on the exciton absorption in the QWR has not been addressed in the literature. Also the problem of electric field ionization of indirect excitons in DQWRs has not been comprehensively studied so far. Thus the analytical multisubband approach to the problem of excitons in uniform nanowires and in DQWRs subjected to both longitudinal magnetic and electric fields is of great interest. Also it is key to the explanation of experimental data to influence and trigger further experiments, and to elucidate the basic physics of the interplay between the autoionization and electric field ionization of the quasi-1D exciton states.

In order to reach these aims and to fill the mentioned gaps concerning the physics of quasi-1D excitons, we develop an analytical approach to the problem of exciton in a cylindrical QWR of radius R bounded by an impenetrable barrier in the presence of longitudinal magnetic B and electric F fields both directed parallel to the QWR axis. Along with the uniform QWR we consider the indirect exciton states in the double QWR formed by two coaxial QWRs in which the electron (e) and hole (h) are spatially separated by an impenetrable insertion of width D. We focus on nanoscaled QWRs of small radius R and strong magnetic field B, providing a significant confinement of the exciton in the transverse plane perpendicular to the QWR axis thereby resulting in a quasi-1D character of the exciton states.

The aims of our calculations are the energies of the indirect exciton in the DQWR and the coefficient of the absorption of light associated with the transitions to the direct exciton states in the UQWR as functions of the confinement (R,a_B) and electric field strength F. In the effective-mass approximation the exciton wave function is expanded with respect to the basis set composed of the transverse wave functions describing the confined lateral motion of the noninteracting electrons and holes. The set of the equations for the longitudinal exciton wave functions is solved for the indirect excitons in the single-subband approximation, and for the direct excitons both in the single- and in the double-subband approximations of two interacting transverse subbands. We demonstrate that our analytical results are in line with those obtained numerically. Estimates of the expected experimental values are made for the parameters of the GaAs/AlGaAs QWR. Let us emphasize that the focus of our approach is to elucidate the basic physics of the exciton states in biased uniform and nonuniform QWRs. We do not intend to compete with the results obtained by comprehensive numerical methods.

The paper is organized as follows. In Sec. II the general approach to the problem, the basis of the lateral functions and the set of equations describing the confined magnetoexciton states in biased QWR are derived. In Sec. III we calculate the complex energy levels relevant to the electric field ionization of the indirect exciton magnetostates in the DQWR. The influence of the electric field ionization, autoionization caused by the intersubband couplings and its combined effect on the exciton magnetoabsorption in the uniform QWR are under consideration in Sec. IV. A discussion of the obtained results, justification of the employed simplifications, as well as a comparison with the available experimental data and estimates of the expected experimental values are provided in Sec. V. Section VI contains the conclusions.

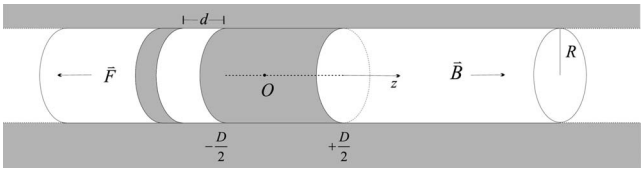

FIG. 1. The DQWR composed of two coaxial QWRs of radius R and quantum disk of height d incorporated in one of the QWRs: QWRs are separated by an insertion of width D.

II. GENERAL APPROACH

We consider a double quantum wire composed of two uniform coaxial cylindrical QWRs separated by an impenetrable insertion of width D (see Fig. 1). Both QWRs are bounded by potential barriers of infinite height at the cylindrical surface of radius R. The magnetic B and electric F fields are chosen to direct parallel to the z axis that in turn coincides with the common axis of the QWRs. The center of the potential barrier separating the QWRs is taken at the point $z=0$. The other length scales relevant to the problem are the exciton Bohr radius a_0 and the magnetic length a_B defined as usual by

$$a_0 = \frac{4\pi\varepsilon_0\varepsilon\hbar^2}{\mu e^2} \quad \text{and} \quad a_B = \left(\frac{\hbar}{eB}\right)^{1/2},$$

where μ is the reduced effective mass of the electron (e) and hole (h) $(\mu^{-1}=m_e^{-1}+m_h^{-1})$, respectively, and ε is the dielectric constant. We take the electron and hole energy bands to be parabolic, nondegenerate, and separated by a wide energy gap E_g.

In the effective-mass approximation the equation describing the indirect exciton formed by the spinless electron and hole having the masses m_j, charges e_j $(e_e=-e_h=-e)$, and positions $\vec{r}_j(\vec{\rho}_j,z_j)$, $(j=e,h)$ subject to the external uniform magnetic $\vec{B}$ and electric $\vec{F}$ fields has the form

$$\left\{\sum_{j=e,h}\left[\frac{1}{2m_j}\left(-i\hbar\vec{\nabla}_j+\frac{e_j}{2}[\vec{B}\times\vec{\rho}_j]\right)^2+e_jFz_j\right]-\frac{e^2}{4\pi\varepsilon_0\varepsilon|\vec{r}_e-\vec{r}_h|}-E\right\}\Psi(\vec{r}_e,\vec{r}_h)=0. \quad (1)$$

By solving this equation subject to the boundary conditions relevant to the indirect exciton

$$\Psi(\vec{\rho}_e,\vec{\rho}_h;z_e,z_h)=0, \quad (2)$$

at any one of the conditions $\rho_e=R$, $\rho_h=R$, $z_e=\frac{1}{2}D$, $z_h=-\frac{1}{2}D$ the total exciton energy E and the wave function Ψ are found in principle. The solution to Eq. (1) can be chosen in the form

$$\Psi(\vec{r}_e,\vec{r}_h)=\sum_l \Phi^{(l)}(\vec{\rho}_e,\vec{\rho}_h)\psi^{(l)}(z_e,z_h), \tag{3}$$

where l is the set of the quantum numbers corresponding to the lateral motion. The transverse basis wave functions $\Phi^{(l)}(\vec{\rho}_e,\vec{\rho}_h)$ obey the equations[17]

$$\left\{\sum_{j=e,h}\frac{1}{2m_j}\left(-i\hbar\vec{\nabla}_j+\frac{e_j}{2}[\vec{B}\times\vec{\rho}_j]\right)^2-E_\perp^{(l)}\right\}\Phi^{(l)}(\vec{\rho}_e,\vec{\rho}_h)=0, \tag{4}$$

and the boundary conditions

$$\Phi^{(l)}(\vec{\rho}_e,\vec{\rho}_h)=0 \quad \text{at any one of two conditions } \rho_e=R,\ \rho_h=R. \tag{5}$$

For the longitudinal wave functions $\psi^{(l)}(z_e,z_h)$ we have

$$\left\{\sum_{j=e,h}\left[-\frac{\hbar^2}{2m_j}\frac{d^2}{dz_j^2}+e_jFz_j\right]-E+E_\perp^{(l)}\right\}\psi^{(l)}(z_e,z_h)+\sum_{l'}V_{ll'}(z_e,z_h)\psi^{(l')}(z_e,z_h)=0, \tag{6}$$

where

$$V_{ll'}(z_e,z_h)=-\frac{e^2}{4\pi\varepsilon_0\varepsilon}\langle l|\frac{1}{\sqrt{(\vec{\rho}_e-\vec{\rho}_h)^2+(z_e-z_h)^2}}|l'\rangle \tag{7}$$

is the matrix element calculated with respect to the functions $\Phi^{(l)}(\vec{\rho}_e,\vec{\rho}_h)$.[15]

For a QWR with arbitrary radius R and magnetic field B, the lateral wave functions $\Phi^{(l)}(\vec{\rho}_e,\vec{\rho}_h)$ and energies $E_\perp^{(l)}$ can be calculated only numerically. However for the limiting cases of strong confinement (quantum wire regime) and of strong magnetic field (magnetic regime), the transverse states can be found analytically.

A. Quantum wire regime ($R \ll a_B$)

In this case the confinement dominates the effect of the magnetic field. The set of the quantum numbers l_j includes the radial N_j and magnetic M_j quantum numbers $l_j \equiv\{N_j,M_j\}$. In the zeroth approximation the normalized transverse wave functions $\Phi^{(l)}(\vec{\rho}_e,\vec{\rho}_h)$, $l\equiv\{l_e,l_h\}$ read

$$\Phi^{(l)}(\vec{\rho}_e,\vec{\rho}_h)=\Phi_{l_e}(\vec{\rho}_e)\Phi_{l_h}(\vec{\rho}_h), \tag{8}$$

where

$$\Phi_{l_e}(\vec{\rho}_e)=\frac{\exp(iM_e\varphi_e)}{\sqrt{2\pi}}\frac{2^{1/2}}{RJ_{|M_e|+1}(\alpha_{|M_e|,N_e})}J_{|M_e|}\left(\alpha_{|M_e|,N_e}\frac{\rho_e}{R}\right). \tag{9}$$

In Eq. (9) $J_{|M|}(x)$ are the Bessel functions, $M=0,\pm1,\pm2,\ldots$ is the magnetic quantum number, and $\alpha_{|M|,N}$ is the root of the Bessel function $[J_{|M|}(\alpha_{|M|,N})=0]$, i.e., $\alpha_{0,1}=2.40$, $\alpha_{0,2}=5.52$, and $\alpha_{1,1}=3.83,\ldots$.[2] Electronic wave function (9) yields the electronic transverse energy

$$E_{\perp l_e}=\frac{\hbar^2\alpha_{|M_e|,N_e}^2}{2m_eR^2}+\frac{\hbar^2}{2m_ea_B^2}M_e+\frac{\hbar^2R^2[2(M_e^2-1)+\alpha_{|M_e|,N_e}^2]}{24m_ea_B^4\alpha_{|M_e|,N_e}^2}. \tag{10}$$

In Eq. (10) the first term is the energy of the carrier in the quantum disk of radius R while others, describing the Zeeman splitting $\sim a_B^{-2}$ and the diamagnetic shift $\sim a_B^{-4}$, are the corrections caused by the magnetic field B. The hole function $\Phi_{l_h}(\vec{\rho}_h)$ and hole transverse energy $E_{\perp l_h}$ can be obtained from Eqs. (9) and (10), respectively, by replacing the index e by index h and taking the complex conjugate. The total transverse energy $E_\perp^{(l)}$ is the sum of the lateral electron and hole energies $E_{\perp l_j}$

$$E_\perp^{(l)}=E_g+E_{\perp l_e}+E_{\perp l_h}. \tag{11}$$

B. Magnetic regime ($a_B \ll R$)

In this case the effect of the strong magnetic field on the radial electron and hole states significantly dominates the effects due to the size quantization in the wide QWR. Neglecting the effect of the confinement suggests introducing a transverse relative coordinate $\vec{\rho}$ and a transverse coordinate of the center of mass $\vec{R}_\perp$

$$\vec{\rho}=\vec{\rho}_e-\vec{\rho}_h;\quad \vec{R}_\perp=\frac{m_e\vec{\rho}_e+m_h\vec{\rho}_h}{m_e+m_h}.$$

For the optically active cylindrically symmetric excitons in question, having a zero magnetic quantum number and zero total momentum, the lateral wave function can be written in the form[32–34]

$$\Phi^{(l)}(\vec{\rho}_e,\vec{\rho}_h)=\frac{\exp\left(\frac{ie}{2\hbar}[\vec{B}\times\vec{\rho}]\cdot\vec{R}_\perp\right)}{\sqrt{S}}\frac{1}{\sqrt{2\pi}a_B}\times\exp\left(-\frac{\rho^2}{4a_B^2}\right)L_N\left(\frac{\rho^2}{2a_B^2}\right), \tag{12}$$

where S is the cross-section square in the x-y plane and where $L_N(x)$, $N=0,1,2,\ldots$ are the Laguerre polynomials. Wave function (12) corresponds to the *electron-hole Landau levels*

$$E_\perp^{(l)}=E_g+\frac{\hbar^2}{2\mu a_B^2}(2N+1);\quad N=0,1,2,\ldots, \tag{13}$$

which become the nondegenerate because of the zero total momentum.

In the absence of the excitonic Coulomb interaction ($V_{ll'}^l=0$), set (6) yields independent equations for different l. The total energy E is the sequence of the electron and hole subbands formed by the branches of the continuous longitudinal energies emanating from the transverse electron and hole energy levels $E_{\perp l_j}$, respectively. The continuous subbands correspond to unbound states of the carriers in the presence of the electric field.

It follows from Eq. (7) that in the region $|z_e-z_h|\gg\bar{\rho}$ ($\bar{\rho}\simeq\langle l|\rho|l\rangle\simeq R$ or a_B)

$$V^l_{l'}(z_e,z_h) \simeq -\frac{e^2}{4\pi\varepsilon_0\varepsilon|z_e-z_h|}\left[\delta_{l,l'}+O\left(\frac{\bar{\rho}^2}{|z_e-z_h|^2}\right)\right].$$

For a narrow QWR and strong magnetic field providing the conditions

$$r_0 \ll a_0 \quad [r_0=\min(R,a_B)], \tag{14}$$

the diagonal potentials V^l_l dominate the off-diagonal potentials, i.e., $V^l_{l'} \sim V^l_l(\bar{\rho}^2/a_0^2)$, $l \neq l'$. In the single-subband approximation we neglect the off-diagonal potentials and only one pair electron-hole subband l_e, l_h is under consideration. In this case set (6) decomposes into independent equations. The 1D exciton states are governed by the quasi-Coulomb $V^l_l(|z_e-z_h|)$ and electric field $eF(z_e-z_h)$ potentials. In the single-subband approximation we encounter a sequence of series of quasidiscrete exciton levels adjacent on the low energy side to the transverse energy level $E^{(l)}_\perp$. In the absence of the electric field all exciton series (l_e,l_h) except the one adjacent to the ground transverse level $E^{(0)}_\perp$ are superimposed on the continuous Coulomb spectra emanating from the lower transverse levels toward the energies $E \geq E^{(l)}_\perp$. Since in the single-subband approximation we neglect the coupling between the bound and unbound exciton states, associated with the different subbands (l_e,l_h), the quasidiscrete character of the exciton levels is caused by the ionization of the 1D exciton states by the electric field F.

In the multisubband approximation in the absence of the electric field the series of the bound exciton states (l_e,l_h) except for the ground series are in resonance with the states of above mentioned continuous spectra, which in turn leads to an autoionization process. In the presence of the electric field an interplay between the autoionization and electric field-ionization process occurs. Below we consider in the single-subband approximation the electric field ionization of the indirect exciton states in the DQWR. The interplay between the electric field ionization and autoionization caused by the intersubband coupling will be studied in the double-subband approximation for the direct excitons in an UQWR ($D=0$, no barrier).

III. INDIRECT EXCITON IN THE DOUBLE QUANTUM WIRE

At this stage we consider (as depicted in Fig. 1) the modified DQWR in which one of the QWR contains the isolated p-doped disk layer positioned close to the interface. A similar structure has been investigated in Ref. 10. Such a structure is appropriate for a study of the spatially separated indirect excitons formed by the holes captured at the interface ($z \simeq -D/2$) and electrons within the semi-infinite QWR ($D/2 \leq z_e \leq \infty$). The polarization of the p-doped layer by the electrons displaces the extra holes in the layer toward the disk-wire interface, which in turn enhances the localization of the exciton hole at $z \simeq -D/2$. The energy of the transverse motion of the exciton hole $\sim \hbar^2/m_h R^2$ exceeds that of the *repulsion between the hole in the exciton and the extra holes in the p-doped layers* $\sim d^{-1}$ under the condition $R^2 < a_h d$, where a_h is the hole Bohr radius. For the holes in the GaAs ($m_h = 0.4m_0$) QWR of radius $R=4.2$ nm, this condition implies $d > 11$ nm. The alternative mechanism to confine the exciton holes near the interface $z=-D/2$ is to create left of the interface the narrow layer with the different electronic parameters, acting as a hole quantum well. This modification does not change qualitatively the physical results, obtained below, but allows to effectively apply the analytical methods and to simplify the numerical calculations. The extension of the obtained results to the arbitrary positioned layer and to the motion of the holes will be given in Sec. V A. In Fig. 1 the region $-\infty \leq z \leq 0$ left of the wire becomes available for the holes in the UQWR ($D \to 0, d \to \infty$).

The longitudinal exciton wave function $\psi^{(l)}(z_e,z_h) = \psi^{(l)}(z_e)\varphi_0(z_h)$ consists of the hole wave function $\varphi_0(z_h)$ describing the hole of the energy E_h within the hole layer and the electron function $\psi^{(l)}(z_e)$. In the single-subband approximation the electron functions $\psi^{(l)}(z_e)$ satisfy Eq. (6) with the diagonal potentials $V^l_l(z_e,z_h)$

$$\psi^{(l)\prime\prime}(u)+\left[\lambda\langle l|(u^2+g^2)^{-1/2}|l\rangle+\frac{\lambda^3 s}{8}u-\frac{1}{4}\right]\psi^{(l)}(u)=0;$$
$$u_0 \leq u \leq \infty, \tag{15}$$

and the boundary conditions

$$\psi^{(l)}(u_0)=0. \tag{16}$$

Equation (15) is written in the terms of the dimensionless electric field s, in-plane g and longitudinal u electron-hole distances, and the quantum number λ, given by the following formulas:

$$u=\frac{2\left(z_e+\frac{1}{2}D\right)}{a_e\lambda}; \quad u_0=\frac{2D}{a_e\lambda}; \quad E-E_g-E^{(l)}_\perp-E_h=-\frac{\mathrm{Ry}^{(e)}}{\lambda^2},$$

$$g^2=\frac{4(\vec{\rho}_e-\vec{\rho}_h)^2}{a_e^2\lambda^2}; \quad s=\frac{eFa_e}{\mathrm{Ry}^{(e)}},$$

$$\text{where } \mathrm{Ry}^{(e)}=\frac{\hbar^2}{2m_e a_e^2} \text{ and } a_e=\frac{4\pi\varepsilon_0\varepsilon\hbar^2}{m_e e^2},$$

are the electron Rydberg constant and the electron Bohr radius, respectively. For an estimation of the parameter g^2 after the integration over the variables $\vec{\rho}_e$ and $\vec{\rho}_h$, we set $(\vec{\rho}_e-\vec{\rho}_h)^2 \simeq r_0^2$, where r_0 is given by Eq. (14). The term $\sim(u^2+g^2)^{-1/2}$ describes the 1D attractive quasi-Coulomb potential, having the asymptotics $\sim|u|^{-1}$ at $|u| \gg g$, $g \ll 1$, finite depth $|g|^{-1}$ at $u=0$, and truncated at the distance $u=u_0$. The solution to Eq. (15) is based on the method developed originally by Hasegawa and Howard (*H-H*) (Ref. 35) and on the method of a comparison equation.[36] The *H-H* method allows taking into account the effect of perturbation of the 1D Coulomb states by the small parameter $g \ll 1$ in the term $\sim(u^2+g^2)^{-1/2}$. The function, calculated by the iteration procedure for $u \ll 1$ and 1D Coulomb function, relevant to the term $\sim|u|^{-1}$ and valid for $|u| \gg g$, are matched in the region $g \ll |u| \ll 1$. The approximate method of a comparison equation is based on replacing the variable u by another one $\xi(u)$, which transforms Eq. (15) to the exact analytically solvable comparison equation. The solution to Eq. (15) is taken in the

form $\psi(u)=[\xi'(u)]^{-1/2}f[\xi(u)]$. Substituting this function into Eq. (15) we arrive at the equation for the variable $\xi(u)$, which in turn allows calculation of the variable $\xi(u)$ itself and the quantum number λ. For the weak electric field s the solutions $f(\xi)$ to the comparison equation are the Whittaker functions.[37] If the effect of the electric field $\sim su$ considerably exceeds that of the Coulomb attraction $\sim|u|^{-1}$, the functions $f(\xi)$ coincide with the Airy functions.[37] Below the Airy functions determine the "outer" wave function, having at large distances u the complex form of an outgoing wave. When matched with the "inner" real function, describing for small distances u the bound state, the complex quantum number λ and consequently the complex energy levels, corresponding to the quasidiscrete states, are found. The imaginary part of these levels $\Gamma/2$ defines the ionization rate $W=\hbar^{-1}\Gamma$, induced by the electric field F. The outgoing wave boundary condition is the key point of the complex energy method (see Ref. 38 for details). The justification of this method and its comparison with others are given in Ref. 26, in which the ionization rate of the 3D hydrogen atom has been calculated. Note that in addition, for example, Eq. (21) will be derived using the comparison equation ignoring the electric field while Eqs. (22) and (41) imply that the electric field is the governing factor.

A. Narrow barrier ($u_0 \ll 1, u_0 \leq g$)

Introducing the left u_1 and right u_2 turning points

$$u_1 = 4\lambda, \quad u_2 = \frac{2}{\lambda^3 s},$$

we sequentially consider Eq. (15) in the classically allowed $u<u_1$, $u>u_2$ and forbidden $u_1<u<u_2$ regions. However, the regions, relevant to the form of the wave function, are $u \ll 1$, $g \ll u \ll u_1$, $u_1<u<u_2$, and $u>u_2$.

1. Region $u<u_1$

In the zeroth approximation we neglect the effect of the electric field $\sim su$ in Eq. (15). In the region $u \ll 1$ an iteration *H-H* method is employed by double integration of Eq. (15) using the following trial function with boundary condition (16)

$$\tilde{\psi}(u) = \alpha(u-u_0)(u^2+g^2)^{1/2}\ln(u+\sqrt{u^2+g^2}),$$

where α is a constant. In the region $u \gg g$ the general solution to Eq. (15) is given by

$$\psi(u) = AW_{\lambda,1/2}(u) + BM_{\lambda,1/2}(u), \tag{17}$$

where $W_{\lambda,1/2}(u)$ and $M_{\lambda,1/2}(u)$ are the Whittaker functions,[37] and A and B are constants. The chosen trial function is the extension of the trial function with $\tilde{\psi}(0)=0$, employed in Ref. 39, to boundary condition (16) at $u_0 \neq 0$, $u_0<g$. The latter in turn is the generalization of the principle u-dependent term $\sim u \ln u$ in the expansion of Eq. (17) at $u \ll 1$ for the case $g \neq 0$, multiplied by the factor u, providing the condition $\tilde{\psi}(0)=0$. The above-given trial function generates the correct solution to Eq. (15) at $u \gg g$, having the terms of the same orders as those of function (17) at $u \ll 1$ and the energy levels transform to the correct 1D Coulomb series $-\mathrm{Ry}^{(e)}/n^2$, $n=1,2,\ldots$, corresponding to the wave functions $\psi_n(z)$ $[\psi_n(0)=0]$ in the limiting case $u_0 \to 0$ and then $g \to 0$. A comparison of the coefficients is then made between the results of double integration taken for $u \gg g$ and the standard expansion of the Whittaker functions involved in Eq. (17) for $u \ll 1$. When terms of the same orders are equated, a set of two linear equations

$$A\frac{1}{\Gamma(-\lambda)} + \alpha\frac{\lambda g^2}{4} = 0 \tag{18}$$

and

$$A\frac{\varphi(\lambda)}{\Gamma(-\lambda)} - \alpha\sqrt{u_0^2+g^2}\ln(u_0+\sqrt{u_0^2+g^2}) + B = 0, \tag{19}$$

results, where

$$\varphi(\lambda) = \psi(1-\lambda) + \frac{1}{2\lambda} + 2\gamma_E - 1, \tag{20}$$

and where $\Gamma(x)$ is the gamma function, $\psi(x)$ is the psi function (the logarithmic derivative of the gamma function), and $\gamma_E \approx 0.577$ is the Euler constant.

The effect of the electric field $\sim s$ on the exciton energy can then be calculated by the method of a comparison equation, in which the comparison equation is the equation for the Whittaker function $W_{\nu,1/2}(\xi)$. The quantum number ν, which defines the exciton energy $-\mathrm{Ry}^{(e)}/\nu^2$ (the Stark effect) can be found from the relationship,[36]

$$\int_{u_0}^{u_1}\left(\frac{\lambda}{u}-\frac{1}{4}\right)^{1/2}du = \int_{u_0}^{u_1}\left(\frac{\nu}{u}-\frac{1}{4}+\frac{\lambda^3 s}{8}u\right)^{1/2}du,$$

to give in turn for the quantum number ν

$$\nu = \lambda\left(1-\frac{3}{4}\lambda^4 s\right), \tag{21}$$

where λ is the unperturbed quantum number, calculated from Eq. (15) at $s=0$.

2. Regions $u_1<u<u_2$ and $u>u_2$

In this region the effect of the electric field $\sim s$ overcomes that of the Coulomb potential, and consequently, as mentioned above, the Airy functions, $Ai(-\xi)$ and $Bi(-\xi)$,[37] occur in the general solution to Eq. (15)

$$\psi(u) = C(\xi')^{-1/2}[Bi(-\xi)+iAi(-\xi)]; \quad \xi(u) = \left[\frac{3}{2}\Theta(u)\right]^{2/3}, \tag{22}$$

where

$$\Theta(u) = \begin{cases} \displaystyle\int_{u_2}^{u}\left(\frac{\lambda}{v}-\frac{1}{4}+\frac{\lambda^3 s}{8}v\right)^{1/2}dv; & u>u_2, \\ \displaystyle -i\int_{u_2}^{u}\left(\frac{-\lambda}{v}+\frac{1}{4}-\frac{\lambda^3 s}{8}v\right)^{1/2}dv; & u<u_2. \end{cases}$$

In the region $u>u_2$ function (22) has the asymptotics of an outgoing wave. Under the condition $s\lambda^4 \ll 1$ functions

(17) and (22) can be matched within the region $u_1 \ll u \ll u_2$. A comparison of Eq. (17) with the Whittaker functions $W_{\lambda,1/2}(u)$ and $M_{\lambda,1/2}(u)$ taken for $u \gg 1$ and Eq. (22) for $u \ll u_2$, $|\Theta| \gg 1$ is made. When terms of the same form are equated, a set of two linear equations results

$$A - B\frac{\cos \pi\lambda}{\Gamma(1+\lambda)} - C\left(\frac{2}{\pi}\right)^{1/2}\tilde{\Phi}^{-1} = 0 \tag{23}$$

and

$$B\frac{1}{\Gamma(1-\lambda)} - \frac{i}{2}C\left(\frac{2}{\pi}\right)^{1/2}\tilde{\Phi} = 0, \tag{24}$$

where

$$\tilde{\Phi} = \exp\left\{-\frac{2}{3\lambda^3 s} - \frac{3}{2}\lambda + \lambda \ln\frac{8}{\lambda^3 s}\right\}. \tag{25}$$

The set of linear algebraic equations (18), (19), (23), and (24) are solved by the determinantal procedure, giving in turn the transcendental equation for the quantum number λ in the form

$$\left[i\frac{\cos \pi\lambda}{2\Gamma(1+\lambda)} + \frac{1}{\tilde{\Phi}^2\Gamma(1-\lambda)}\right]\left[q_l + \frac{(g^2)_l}{4}\lambda\varphi(\lambda)\right] - i\frac{(g^2)_l}{8}\Gamma(1-\lambda) = 0, \tag{26}$$

where the function $\varphi(\lambda)$ is given by Eq. (20) and where

$$q_l = \langle l|(u_0^2+g^2)^{1/2}\ln(u_0+\sqrt{u_0+g^2})|l\rangle, \quad (g^2)_l = \langle l|g^2|l\rangle.$$

Solving Eq. (26), the quantum number λ and then ν and the exciton energy E in Eq. (15) can be obtained as a function of the magnetic field B and/or radius of the QWR R $[(g^2)_l]$, electric field $F(s)$, and the width of the interwire barrier $D(u_0)$.

The limiting case of a vanishing electric field $F=s=0$ [Eq. (26)] for $\tilde{\Phi}=0$ reads

$$\varphi(\lambda) + \frac{4q_l}{\lambda(g^2)_l} = 0,$$

giving for the quantum number λ

$$\lambda = n + \delta_n; \quad n = 1,2,3,\ldots; \quad \delta_n = -\frac{n(g^2)_l}{4q_l}. \tag{27}$$

The quantum defect $\delta_n \ll 1$ describes the blue energy shift of the exciton state n caused by the confinement (strong magnetic field B and/or QWR radius R) and the finite width D of the interwire barrier. This blueshift reflects the reduction in the exciton binding energy, which is the result of the finite depth of the quasi-Coulomb well $\sim -(u^2+g^2)^{-1/2}$ at $u=0$ and excluding the region $0 \le u \le u_0$ [see Eq. (16)] within which electron-hole attraction is significant. In the limiting case of an extremely strong confinement {very small radius of the QWR or very intensive magnetic field $[(g^2)_l \to 0]$} and a very narrow interwire barrier $D(u_0 \to 0)$, we obtain from Eq. (26) at $q_l=(g^2)_l=0$

$$i\frac{\cos \pi\lambda}{2\Gamma(1+\lambda)}\tilde{\Phi}^2 + \frac{1}{\Gamma(1-\lambda)} = 0. \tag{28}$$

The solution to this equation is

$$\lambda = n + i\Delta_n; \quad \Delta_n = -\frac{1}{2n!\,(n-1)!}\tilde{\Phi}^2, \tag{29}$$

in which $\lambda = n = 1,2,3,\ldots$ should be taken in Eq. (25) for $\tilde{\Phi}$. The imaginary part of the quantum defect $\Delta_n \ll 1$ reflects the width of the quasidiscrete exciton energy level n associated with the ionization of the exciton state by the electric field F. In principle, the factor $\tilde{\Phi}^2$ can be found calculating the tunneling probability of the particle having the energy $-\mathrm{Ry}^{(e)}/\lambda^2$ via the 1D potential barrier formed by the Coulomb potential $\sim -u^{-1}$ and the potential due to the uniform electric field $\sim -su$.

B. Intermediate barrier ($u_0 \ll 1, u_0 \gg g$)

Neglecting the parameter g in the term $\sim(u^2+g^2)^{-1/2}$ in Eq. (15), we arrive at general solution (17) to this equation in the region $u_0 \le u \ll u_2$. Boundary condition (5) for function (17) at $u_0 \ll 1$ gives

$$A\frac{\chi(\lambda)}{\Gamma(-\lambda)} + B = 0, \tag{30}$$

where

$$\chi(\lambda) = \varphi(\lambda) - \frac{1}{\lambda u_0} + \ln u_0. \tag{31}$$

The set of linear algebraic equations (23), (24), and (30) is then again solved by the determinantal method, and provides the transcendental equation

$$\left[i\frac{\cos \pi\lambda}{2\Gamma(1+\lambda)} + \frac{1}{\tilde{\Phi}^2\Gamma(1-\lambda)}\right]\chi(\lambda) + \frac{i}{2}\Gamma(-\lambda) = 0. \tag{32}$$

In the absence of the electric field Eq. (32) transforms into the equation $\chi(\lambda)=0$, where $\chi(\lambda)$ and $\varphi(\lambda)$ are given by Eqs. (31) and (20), respectively. In particular in the logarithmic approximation $|u_0 \ln u_0| \ll 1$ the quantum number λ relevant to the zeroth electric field $F=0$ is given by

$$\lambda = n + \delta_n; \quad \delta_n = nu_0; \quad n = 1,2,\ldots. \tag{33}$$

Similar to Eq. (27) the quantum defect $\delta_n \ll 1$ [Eq. (33)] shows a blueshift of the exciton state n induced by the width D of the interwire barrier. The corresponding reduction in the binding energy $\Delta E \sim -(\mathrm{Ry}^{(e)}/n^2)u_0$ is the consequence of the shortening of the region available for the exciton motion by the amount $0 \le u \le u_0$. The given above energy shift ΔE can be estimated by the integration of Eq. (15) for $g=s=0$ over the region $u_0 \le u \le \infty$ using the ground-state $(n=1)$ wave function $\psi(u) \sim u\exp(-u/2)$. Setting formally $u_0 \to 0$ $[\chi(\lambda) \to \infty]$ in Eq. (32) we arrive at Eq. (28) and quantum number (29).

C. Wide barrier ($u_0 \ge 1$)

In the absence of the electric field the general solution to Eq. (15) can be obtained from Eq. (17) for $B=0$. Boundary

condition (5) for function (17) at $B=0$ leads to the equation for the quantum number λ

$$W_{\lambda,1/2}(u_0)=0. \tag{34}$$

For the excited levels ($\lambda \gg 1$) we have from Eq. (34)

$$\lambda = N + \frac{2u_0}{\pi^2} + 2\frac{u_0^{1/2}}{\pi}\sqrt{\frac{u_0}{\pi^2}+N} = \begin{cases} N\left(1+\frac{2}{\pi}\frac{u_0^{1/2}}{N^{1/2}}\right); & \frac{\pi^2 N}{u_0} \gg 1, \\ 4\frac{u_0}{\pi^2}\left(1+\frac{N\pi^2}{2u_0}\right); & \frac{\pi^2 N}{u_0} \ll 1, \end{cases} \quad N \equiv n - \frac{1}{4}, \tag{35}$$

and then arrive at the energy levels in a strongly truncated ($D > a_e$) Coulomb potential. Clearly the wide interwire barrier leads to a considerable decrease in exciton binding energy and the exciton states appear to be completely ionized even for a small electric field.

IV. DIRECT EXCITON IN THE UNIFORM QUANTUM WIRE

Here we consider a direct exciton formed by the electron and hole in the UQWR ($-\infty \le z_{e,h} \le +\infty$). The total exciton wave function $\Psi(\vec{r}_e,\vec{r}_h)$ for the zeroth longitudinal total momentum can be chosen in the form

$$\Psi(\vec{r}_e,\vec{r}_h) = \frac{1}{\sqrt{L}}\sum_l \Phi^{(l)}(\vec{\rho}_e,\vec{\rho}_h)\psi^{(l)}(z); \quad z = z_e - z_h, \tag{36}$$

where L is the macroscopic length of the QWR, and where the transverse basis wave functions $\Phi^{(l)}(\vec{\rho}_e,\vec{\rho}_h)$ are given by Eqs. (8), (9), and (12). The functions $\psi^{(l)}(z)$ describing the relative longitudinal exciton motion obey the equations

$$-\frac{\hbar^2}{2\mu}\frac{d^2\psi^{(l)}(z)}{dz^2} - [eFz + E - E_\perp^{(l)}]\psi^{(l)}(z) + \sum_{l'} V_{l'}^{l}(z)\psi^{(l')}(z) = 0, \tag{37}$$

where E is the total exciton energy and $E_\perp^{(l)}$ is the energy of the transverse motion determined by Eqs. (11), (10), and (13). The potentials $V_{l'}^{l}(z)$ are given by the right-hand part of Eq. (7) in which $z_e - z_h \equiv z$.

It was justified originally in Ref. 40 that the exciton absorption can be treated as the optical transition of an electron-hole pair from the ground state described by the wave function $\Psi^{(0)}(\vec{r}_e,\vec{r}_h)=\delta(\vec{r}_e-\vec{r}_h)$ to the excited state, corresponding to exciton function (36). The coefficient of absorption $\alpha(\omega)$, where $\omega=E/\hbar$ is the frequency of the absorbed photon, is defined by the overlap integral between these functions, which establish the selection rules for the interband transitions. In the magnetic regime ($a_B \ll R$) the transitions are allowed in the cylindrically symmetric transverse states (12) with the magnetic quantum number $M=0$ and $N=0,1,2,\ldots$. In the QWR regime ($R \ll a_B$) only the states (9) having the same axial symmetry ($M_e=M_h=M=0,\pm 1,\pm 2,\ldots$) and the numbers of the subbands $N_e=N_h=N=1,2,\ldots$ are involved in the interband transitions. Here we take for the coefficient of the exciton absorption

$$\alpha(\omega) = \frac{1}{r_0^2}\begin{cases} \left|\sum_{N=0}^{\infty}\psi^{(N)}(0)\right|^2; & r_0 = a_B \text{ for the magnetic regime}, \\ \left|\sum_{M=0,N=1}^{\infty}\psi^{(M,N)}(0)\right|^2; & r_0 = R \text{ for the QWR regime}. \end{cases} \tag{38}$$

A. Single-subband approximation

In the single-subband (SS) approximation the equation for the longitudinal exciton function $\psi^{(l)}(z)$ corresponding to the quasidiscrete state can be found from Eq. (37) for $V_{l'}^{l}=V_l^l\delta_{l,l'}$. We arrive at Eq. (15) with

$$u = \frac{2z}{a_0\lambda}; \quad E - E_g - E_\perp^{(l)} = W = -\frac{\mathrm{Ry}^{(\mathrm{ex})}}{\lambda^2}; \quad \mathrm{Ry}^{(\mathrm{ex})} = \frac{\hbar^2}{2\mu a_0^2}; \quad -\infty \le u \le +\infty.$$

In the region $u \ll 1$, an iteration method is employed by double integration of Eq. (15) using the trial function $\tilde{\psi}(u)=\beta$, $\tilde{\psi}'(0)=0$ satisfying the boundary conditions for the optically active excitons [Eq. (38)] for which $\tilde{\psi}(0)\neq 0$. Note that under the condition $g \ll 1$ the additional terms in the trial function $\tilde{\psi}(u)$, providing the derivative $\tilde{\psi}'(u)\neq 0$, lead to negligibly small corrections to the effects calculated with the chosen trial function. In the region $u \gg g$ the general solution to Eq. (15) is given by Eq. (17). A comparison of the function obtained by the double integration for $u \gg g$ with the conditions imposed on the trial function and its derivative, and that calculated from Eq. (17) for $u \ll 1$ (Ref. 37) leads to the set of two equations

$$A\frac{1}{\Gamma(1-\lambda)}-\beta=0, \tag{39}$$

$$A\frac{\varphi(\lambda)}{\Gamma(-\lambda)}+\beta\lambda[\ln 2-1-(\ln g)_l]+B=0. \tag{40}$$

In contrast to Sec. III here we treat the quasidiscrete exciton state as a real state of the real energy of the continuous spectrum possessing a maximum of the energy-level density. In the regions $u_1<u<u_2$ and $u>u_2$ we replace complex solution (22) possessing the asymptotic of an outgoing wave by the real function with the asymptotic of a standing wave

$$\psi(u)=C(\xi')^{-1/2}[Bi(-\xi)\cos\vartheta+Ai(-\xi)\sin\vartheta];$$

$$C=\frac{\sqrt{\mu a_0\lambda}}{\hbar}. \tag{41}$$

Wave function (41) is normalized according to $\delta(W-W')$ following the well-known rule, related to the flux density. As above under the condition $s\lambda^4\ll 1$ in the region $u_1\ll u\ll u_2$, we match the asymptotic expansions of functions (17) at $u\gg 1$ and (41) at $|\Theta|\gg 1$.[37] A set of two linear equations reads

$$A-B\frac{\cos\pi\lambda}{\Gamma(1+\lambda)}-C\left(\frac{2}{\pi}\right)^{1/2}\tilde{\Phi}^{-1}\cos\vartheta=0, \tag{42}$$

$$B\frac{1}{\Gamma(1-\lambda)}-C\frac{1}{2}\left(\frac{2}{\pi}\right)^{1/2}\tilde{\Phi}\sin\vartheta=0, \tag{43}$$

where $\tilde{\Phi}$ is given by Eq. (25).

Solving the set of equations (39)–(43) by the determinantal method, we arrive at the equation for the phase ϑ

$$\cot\vartheta=\frac{\tilde{\Phi}^2}{2}\frac{\Gamma^2(1-\lambda)}{\lambda}\left[\frac{1}{\zeta_l(\lambda)}-\frac{\sin 2\pi\lambda}{2\pi}\right], \tag{44}$$

and for the coefficient of exciton absorption (38)

$$\alpha^{(l)}(\omega)=|\beta|^2=\frac{\mu a_0\lambda}{2\pi\hbar^2 r_0^2}\tilde{\Phi}^2\frac{\Gamma^2(-\lambda)}{\zeta_l^2(\lambda)}\left\{1+\frac{\tilde{\Phi}^4}{4}\frac{\Gamma^4(1-\lambda)}{\lambda^2}\times\left[\frac{1}{\zeta_l(\lambda)}-\frac{\sin 2\pi\lambda}{2\pi}\right]^2\right\}^{-1}, \tag{45}$$

where

$$\zeta_l(\lambda)=\psi(1-\lambda)+\frac{1}{2\lambda}+\left(\ln\frac{g}{2}\right)_l+2\gamma_E. \tag{46}$$

Equation (45) describes the exciton absorption as a function of the photon energy $E=\hbar\omega$ [$\lambda=\lambda(E)$].

1. Exciton electroabsorption

We refer to the exciton electroabsorption as the optical absorption caused by the transitions to the quasidiscrete exciton states. In the vicinity of the resonant energy, determined by the quantum number λ_n calculated from

$$\zeta_l(\lambda_n)=0;\quad \lambda_n=n+\Delta_n;\quad \Delta_n<1;\quad n=0,1,2,\ldots. \tag{47}$$

Equation (45) may be rearranged to

$$\alpha^{(l)}(\omega,n)=\alpha_0(n)\Lambda^{(l)}(\omega,n), \tag{48}$$

where

$$\alpha_0(n)=\frac{2\mu a_0\lambda \mathrm{Ry}^{(\mathrm{ex})}}{\hbar^2 r_0^2\lambda_n^4\left|\frac{\partial\zeta_l}{\partial\lambda}\right|}; \tag{49}$$

$$\Lambda^{(l)}(\omega,n)=\frac{\Gamma^{(l)}(n)}{2\pi\left\{[\hbar\omega-E_{\mathrm{ex}}^{(l)}(n)-\Delta E^{(l)}(n)]^2+\frac{\Gamma^{(l)2}(n)}{4}\right\}}.$$

The energy

$$E_{\mathrm{ex}}^{(l)}(n)=E_g+E_\perp^{(l)}-\frac{\mathrm{Ry}^{(\mathrm{ex})}}{\lambda_n^2};\quad n=0,1,2,\ldots,$$

are the strictly discrete energy levels of the quasi-1D exciton in the absence of the electric field. We omit here the linear and squared Stark terms for the excited $n=1,2,\ldots$, and the ground $n=0$ levels of the orders $sn^4\ll 1$ and $s^2\lambda_0^6\ll 1$, respectively (see Ref. 41 for details). Note that the state $n=0$ is relevant only to the direct exciton in contrast to the indirect exciton [see Eqs. (27) and (33)] because of imposed boundary condition (16). These levels can be found from Eqs. (39) and (40) at $B=0$. The width $\Gamma^{(l)}(n)$ and the shift $\Delta E^{(l)}(n)$ of the optical peak caused by the electric field F ionization of the exciton

$$\Gamma^{(l)}(n)=-\frac{4\pi\mathrm{Ry}^{(\mathrm{ex})}}{\lambda_n^3\left(\frac{\partial\zeta_l}{\partial n}\right)}\frac{\sin 2\delta_n}{\sin 2\pi\lambda_n}, \tag{50}$$

$$\Delta E^{(l)}(n)=\frac{4\pi\mathrm{Ry}^{(\mathrm{ex})}}{\lambda_n^3\left(\frac{\partial\zeta_l}{\partial n}\right)}\frac{\cos^2\delta_n}{\sin 2\pi\lambda_n}, \tag{51}$$

can be written in terms of the parameter δ_n, where

$$\cot\delta_n=\frac{1}{2}\tilde{\Phi}^2\frac{\Gamma(1-\lambda_n)}{\Gamma(1+\lambda_n)}\cos\pi\lambda_n. \tag{52}$$

As will be discussed in Sec. V B the energies $E_{\mathrm{ex}}^{(l)}(n)$, $\Delta E^{(l)}(n)$, and widths $\Gamma^{(l)}(n)$ can also be found as the real and imaginary parts of the complex energies of the quasidiscrete states, using the method employed in Sec. III. Below we focus on the effect of the electric field F on the width of the exciton peak $\Gamma^{(l)}(n)$ [Eq. (50)] and on the maximum of the exciton absorption $\alpha_{\max}^{(l)}(\omega,n)$ [Eq. (48)].

a. Ground state $n=0$, $\lambda_0=\Delta_0<1$. It follows from Eqs. (46), (47), and (52) that in the logarithmic approximation $g|\ln g|\ll 1$ and under the condition $\tilde{\Phi}^4/4\ll 1$

$$\Delta_0\simeq-\frac{1}{2\ln g};\quad \frac{\partial\zeta}{\partial n}\simeq-\frac{1}{2\Delta_0^2};$$

$$\cos\ \delta_0 \simeq \frac{\tilde{\Phi}^2}{2}\cos\ \pi\Delta_0; \quad \sin\ \delta_0 \simeq 1,$$

which provides for the width [Eq. (50)] and for the maximum absorption [Eqs. (48) and (49)] at $\hbar\omega_0 = E_{\mathrm{ex}}^{(l)}(0) + \Delta E^{(l)}(0)$,

$$\Gamma^{(l)}(0) = \frac{4\mathrm{Ry}^{(\mathrm{ex})}\tilde{\Phi}^2}{\Delta_0^2}; \quad \alpha_{\max}^{(l)}(\omega_0) = \frac{\mu a_0 \Delta_0}{2\pi r_0^2 \hbar^2 \tilde{\Phi}^2}. \tag{53}$$

b. Excited states $n=1,2,\ldots$, $\lambda_n = n+\Delta_n$, $\Delta_n < 1$. Under the same conditions as those used for the ground state $n=0$, we have from Eqs. (46), (47), and (52)

$$\Delta_n \simeq -\frac{1}{\ln g}; \quad \frac{\partial\zeta}{\partial n} \simeq -\frac{1}{\Delta_n^2};$$

$$\cos\ \delta_n \simeq \frac{\tilde{\Phi}^2}{2n\,!\,(n-1)\,!\,\Delta_n}; \quad \sin\ \delta_n \simeq 1.$$

The width [Eq. (50)] and maximum absorption [Eqs. (48) and (49)] for $\hbar\omega_n = E_{\mathrm{ex}}^{(l)}(n) + \Delta E^{(l)}(n)$ become

$$\Gamma^{(l)}(n) = \frac{2\mathrm{Ry}^{(\mathrm{ex})}\tilde{\Phi}^2}{n^2 n!^2}; \quad \alpha_{\max}^{(l)}(\omega_n) = \frac{\mu a_0 n\,!\,(n-1)\,!\,\Delta_n^2}{2\pi r_0^2 \hbar^2 \tilde{\Phi}^2}. \tag{54}$$

As above, the width $\Gamma^{(l)}(n)$ and shift $\Delta E^{(l)}(n)$ of the exciton peaks, determined by Eqs. (25) and (50)–(54), are induced by the electron-hole tunneling via the potential barrier formed by the Coulomb and electric field potentials. In the absence of the electric field $F=0$, $\tilde{\Phi}=0$, Eqs. (48) and (49) transform into the sequence of the δ-function-type form exciton peaks $\alpha^{(l)}(\omega,n) = \alpha_0(n)\delta[\hbar\omega - E_{\mathrm{ex}}^{(l)}(n)]$.

2. Franz-Keldysh exciton effect

Here we consider the exciton effect on the optical electroabsorption below the threshold at the energies $\hbar\omega - E_g - E_\perp^{(l)} = W_l < 0$ positioned far away from the exciton peaks $[|\hbar\omega - E_g - E_\perp^{(l)} + \mathrm{Ry}^{(\mathrm{ex})}/\lambda_n^2| \gg \Gamma^{(l)}(n)]$. Since the quantum number λ is significantly different from that corresponding to the exciton level n [Eq. (47)] $(\lambda \neq \lambda_n = n+\Delta_n)$, the factor $\Gamma(1-\lambda)\Gamma(-\lambda)\zeta_l^{-1}(\lambda)$ in the denominator of Eq. (45) does not have singularities. Under the condition $\tilde{\Phi}^4 \ll 1$ results

$$\alpha^{(l)}(\omega) = \alpha_{F\text{-}K}(\omega)\frac{\Gamma^2(-\lambda)}{4\zeta_l^2(\lambda)}\exp\left[3\lambda\ \ln\frac{4}{\lambda^2 c}\right],$$

$$\lambda = \left(\frac{\mathrm{Ry}^{(\mathrm{ex})}}{|W_l|}\right)^{1/2}; \quad c = \frac{W_F}{\mathrm{Ry}^{(\mathrm{ex})}}, \quad W_F = \left(\frac{\hbar^2 e^2 F^2}{2\mu}\right)^{1/3}, \tag{55}$$

where

$$\alpha_{F\text{-}K}(\omega) = \frac{1}{\pi r_0^2}\left(\frac{2\mu}{\hbar^2|W_l|}\right)^{1/2}\exp\left[-\frac{4}{3}\left(\frac{|W_l|}{W_F}\right)^{3/2}\right] \tag{56}$$

is the coefficient of the electroabsorption in the 1D structure associated with the photon-assisted interband tunneling of the free carriers (Franz-Keldysh effect) in the region $|W_l| \gg W_F$. The factor $\alpha^{(l)}(\omega)/\alpha_{F\text{-}K}^{(l)}(\omega)$ in Eq. (55) describes the exciton effect on the electroabsorption induced by the transitions to the unbound electron-hole states [Eq. (56)]. It follows from Eq. (46) that if the energy shift $|W_l|$ significantly exceeds the exciton Rydberg constant $\mathrm{Ry}^{(\mathrm{ex})}$ $[\lambda \ll 1, \Gamma(-\lambda) = 2\zeta(\lambda)]$ then the exciton interaction has little effect and $\alpha^{(l)}(\omega) = \alpha_{F\text{-}K}^{(l)}(\omega)$.

B. Double-subband approximation

As mentioned above, in the magnetic regime $(a_B \ll R)$ only the cylindrically symmetric transverse states [Eq. (12)] with the magnetic quantum number $M=0$ are optically active, and in Eq. (36) the index l coincides with the quantum number $N=0,1,2,\ldots$. Since in Eq. (37) the off-diagonal potentials [Eq. (7)] obey $V_0^1(z) = V_1^0(z) \neq 0$ the closest Landau subbands $l'=N=0$ and $l=N=1$ are involved in the double-subband (DS) approximation. For the QWR regime $(R \ll a_B)$ we keep, in Eq. (36), closest transverse states (8) and (9) $l=\{l_e;l_h\} \equiv \{M_e,N_e;M_h,N_h\}$ with $M_{e,h}=0,1$, $N_{e,h}=1$. However, only for the states $l'=\{0,1;0,1\}$, $l=\{1,1;1,1\}$ the off-diagonal potentials $V_{l'}^{l}(z) = V_l^{l'}(z)$ are nonvanishing. The size-quantized closest subbands $l'=0$ and $l=1$ are those which contribute to the DS approximation. This approximation has been developed originally in Ref. 42 and successfully applied to the resonant exciton states in a quantum well[43] and superlattice.[44]

The set of equations (37) describing the coupling between the discrete and continuous exciton states of the energies $E_\perp^{(0)} < E < E_\perp^{(1)}$ adjusted to the first-excited electron-hole subband $l=1$ and branching from the ground subband $l=0$, respectively, can be written in the form

$$\psi^{(1)\prime\prime}(u) + \left[\lambda\langle 1|\frac{1}{\sqrt{g^2+u^2}}|1\rangle + f_1 u - \frac{1}{4}\right]\psi^{(1)}(u) + \lambda\langle 1|\frac{1}{\sqrt{g^2+u^2}}|0\rangle\psi^{(0)}(u) = 0, \tag{57}$$

$$\psi^{(0)\prime\prime}(v) + \left[k\langle 0|\frac{1}{\sqrt{p^2+v^2}}|0\rangle + f_0 v + \frac{1}{4}\right]\psi^{(0)}(v) + k\langle 0|\frac{1}{\sqrt{p^2+v^2}}|1\rangle\psi^{(1)}(v) = 0. \tag{58}$$

In the above equations the following notations have been made

$$u = \frac{2z}{a_0\lambda}; \quad g^2 = \frac{4(\vec{\rho}_e - \vec{\rho}_h)^2}{a_0^2\lambda^2};$$

$$f_1 = \frac{eFa_0\lambda^3}{8\mathrm{Ry}^{(\mathrm{ex})}}; \quad E - E_\perp^{(1)} = -\frac{\mathrm{Ry}^{(\mathrm{ex})}}{\lambda^2}.$$

The variable v, parameter p^2, and dimensionless electric field f_0 can be obtained from the variable u, parameter g^2, and field f_1 by replacing λ by k, where the quantum number k is found from equation $E-E_{\perp}^{(0)}=\mathrm{Ry}^{(\mathrm{ex})}/k^2$. The quantum numbers obey the relationship

$$\frac{1}{\lambda^2}+\frac{1}{k^2}=\frac{E_{\perp}^{(1)}-E_{\perp}^{(0)}}{\mathrm{Ry}^{(\mathrm{ex})}}\equiv G^2\gg 1. \tag{59}$$

Since the matching procedure of solving the sets (57) and (58) closely resembles that used in Sec. IV A, only an outline of the calculations will be given below. Comparing the functions $\psi^{(1)}(u)$ obtained by the double integration of Eq. (57) with the trial functions $\tilde{\psi}^{(1,0)}(u)=\beta_{1,0}$ and by the expansion of Eq. (17) in the region $g\ll u\ll 1$, we arrive at Eq. (39) with $\beta\equiv\beta_1$ and at the following expression

$$A\frac{\varphi(\lambda)}{\Gamma(-\lambda)}+\beta_1\lambda[\ln 2-1-(\ln g)_1]+B-\beta_0\lambda\overline{\ln g}=0;$$

$$\overline{\ln g}=\langle 0|\ln g|1\rangle. \tag{60}$$

As above accomplished, matching the solutions (17) and (41) to Eq. (57) in the region $1\ll u\ll u_2$ gives the set of equations (42) and (43).

For $v\gg p$ we take the general solution to Eq. (58) in the form

$$\psi^{(0)}(v)=D[e^{i\Lambda}W_{ik,1/2}(-iv)+e^{-i\Lambda}W_{-ik,1/2}(iv)]. \tag{61}$$

Note that Eq. (61) describes the effect of the electric field on the continuous exciton state while Eq. (17) corresponds to the electric field ionization of the discrete exciton state. Comparing the functions $\psi^{(0)}(v)$ obtained by the double integration of Eq. (58) and by the expansion of Eq. (61) in the region $p\ll v\ll 1$, the set of equations results

$$\beta_0+2D\left(\frac{\sinh\pi k}{\pi k}\right)^{1/2}\sin[\Lambda+\sigma(k)]=0;\quad \sigma(k)=\arg\Gamma(ik), \tag{62}$$

$$\beta_0[\ln 2-1-(\ln p)_0]+2D\left(\frac{\sinh\pi k}{\pi k}\right)^{1/2}\sin[\Lambda+\sigma(k)]\times\left[\frac{1}{2}[\psi(1+ik)+\psi(1-ik)]-\frac{\pi}{1-e^{-2\pi k}}\cot[\Lambda+\sigma(k)]+2\gamma_E-1\right]-\beta_1\overline{\ln p}=0;\quad \overline{\ln p}=\langle 1|\ln p|0\rangle. \tag{63}$$

In the region v where the Coulomb potential $\sim v^{-1}$ has little effect, the wave function $\psi^{(0)}(v)$ can be obtained from Eqs. (22) and (41) by replacing u by v, λ by k, $-1/4$ by $+1/4$, and u_2 by $v_2=-(4f_0)^{-1}$. Comparing this function and function (61) in the region $1\ll|v|\ll|v_2|$, we find for the coefficient D and the phase Λ

$$D=\frac{1}{(2\pi)^{1/2}}\frac{\sqrt{\mu a_0 k}}{\hbar}e^{-\pi k/2};\quad \Lambda=\frac{|v_2|}{3}-k\ln 4|v_2|+\frac{\pi}{4}-\vartheta. \tag{64}$$

Solving the set of equations (39) for $\beta\equiv\beta_1$ and (42)–(63) with respect to the coefficients β_0, β_1, A, B, C, D by the determinantal method, we obtain the equation for the phase ϑ

$$\left[\frac{\sin 2\pi\lambda}{2\pi}+\frac{2\lambda\cot\vartheta}{\Gamma^2(1-\lambda)\tilde{\Phi}^2}\right]\left[\zeta_1(\lambda)-\frac{\overline{\ln g}\,\overline{\ln p}}{\eta_0(k)-\frac{\pi}{1-e^{-2\pi k}}\cot Q}\right]-1=0. \tag{65}$$

In Eq. (65) $\zeta_1(\lambda)$ is given by Eq. (46) for $l=1$, $\tilde{\Phi}$ by Eq. (25), and

$$\eta_0(k)=\frac{1}{2}[\psi(1+ik)+\psi(1-ik)]+\left(\ln\frac{p}{2}\right)_0+2\gamma_E,$$

$$Q(k)=\sigma(k)+\frac{2}{3k^3s}-k\ln\frac{8}{k^3s}+\frac{\pi}{4}-\vartheta;\quad s=\frac{eFa_0}{\mathrm{Ry}^{(\mathrm{ex})}}.$$

The same set gives for the coefficient of exciton absorption (38) two alternative forms

$$\alpha(\omega)=\frac{1}{r_0^2}|\beta_0+\beta_1|^2=\frac{2\mu a_0 k}{\pi\hbar^2 r_0^2}e^{-\pi k}\left(\frac{\sinh\pi k}{\pi k}\right)\sin^2 Q\times\left\{1-\frac{\eta_0(k)-\frac{\pi}{1-e^{-2\pi k}}\cot Q}{\overline{\ln p}}\right\}^2, \tag{66}$$

$$\alpha(\omega)=\frac{1}{r_0^2}|\beta_0+\beta_1|^2=\frac{2\mu a_0\lambda}{\pi\hbar^2 r_0^2}\tilde{\Phi}^2\sin^2\vartheta\frac{\Gamma^2(-\lambda)}{4}\times\frac{1}{\left\{\zeta_1(\lambda)-\frac{\overline{\ln g}\,\overline{\ln p}}{\eta_0(k)-\frac{\pi}{1-e^{-2\pi k}}\cot Q}\right\}^2}\times\left\{1-\frac{\overline{\ln p}}{\eta_0(k)-\frac{\pi}{1-e^{-2\pi k}}\cot Q}\right\}^2. \tag{67}$$

In the limiting case of neglecting intersubband coupling $\overline{\ln g}=\overline{\ln p}=0$ Eqs. (65) and (67) lead to Eq. (45) describing the exciton electroabsorption [Eqs. (48) and (49)] and Franz-Keldysh effect [Eq. (55)] in the single-subband approximation. In the absence of the electric field $F=\tilde{\Phi}=0$ Eqs. (65) and (66) provide the coefficient of the exciton absorption

$$\alpha(\omega)=\frac{2\mu a_0 k}{\pi\hbar^2 r_0^2}e^{-\pi k}\left(\frac{\sinh\pi k}{\pi k}\right)\left(1-\frac{\overline{\ln g}}{\zeta_1(\lambda)}\right)^2\times\left\{1+\left(\frac{1-e^{-2\pi k}}{\pi}\right)^2\left(\eta_0(k)-\frac{\overline{\ln g}\,\overline{\ln p}}{\zeta_1(\lambda)}\right)^2\right\}^{-1}. \tag{68}$$

In the vicinity of the resonant exciton state (Fano resonances[25]) determined by the quantum numbers $\lambda_n=n+\Delta_n$, $n=0,1,2,\ldots$ calculated from $\zeta_1(\lambda_n)=0$ [Eq. (47)], Eq. (68) transforms into Eq. (48) with

$$\alpha_0(n) = \frac{2}{a_0 r_0^2 \lambda^3 \left| \frac{\partial \zeta_1(\lambda)}{\partial \lambda} \right|} \frac{\overline{\ln g}}{\overline{\ln p}};$$

$$\frac{\partial \zeta_1(\lambda)}{\partial \lambda} = \begin{cases} -(2\Delta_0^2)^{-1}, & n=0;\ \Delta_0 = -[2(\ln g)_1]^{-1}, \\ -\Delta_n^{-2}, & n=1,2,\ldots;\ \Delta_1 = -[(\ln g)_1]^{-1}, \end{cases} \tag{69}$$

and Lorentzian profile (49). In Eq. (69) the derivative $\frac{\partial \zeta_1(\lambda)}{\partial \lambda}$ and quantum defects $\Delta_{0,1}$ are given in the logarithmic approximation $|(g)_1(\ln g)_1| \ll 1$.

The corresponding resonance width $\Gamma(n)$ and shift $\Delta E(n)$ in Eq. (49) both caused by the intersubband 0–1 coupling become

$$\Gamma(n) = -\frac{4\mathrm{Ry}^{(\mathrm{ex})}}{\lambda^3 \frac{\partial \zeta_1(\lambda)}{\partial \lambda}} \frac{1 - e^{-2\pi k}}{\pi} \overline{\ln g}\ \overline{\ln p}\ \sin^2 \gamma_n, \tag{70}$$

$$\Delta E(n) = \frac{\mathrm{Ry}^{(\mathrm{ex})}}{\lambda^3 \frac{\partial \zeta_1(\lambda)}{\partial \lambda}} \frac{1 - e^{-2\pi k}}{\pi} \overline{\ln g}\ \overline{\ln p}\ \sin 2\gamma_n, \tag{71}$$

where

$$\cot \gamma_n = \eta_0(k) \frac{1 - e^{-2\pi k}}{\pi}.$$

Exciton absorption (48) with profile (49), width (70), and shift (71) obtained above as the limiting case for $F=0$ from the general equations (65)–(67) coincides completely with that calculated in Ref. 42 in which the exciton magnetoabsorption in bulk material has been studied originally in the double-Landau subband approximation.

Below we present the explicit expressions for the parameters relevant to the problem in the quantum wire regime ($R \ll a_B$)

$$(\ln g)_{0,1} = \ln \frac{2R}{a_0 \lambda} + C_{0,1},$$

$$C_0 = \frac{2}{J_1^2(\alpha_{01})} \int_0^1 x \ln x J_0^2(\alpha_{01} x) dx = -1,$$

$$C_1 = \frac{2}{J_2^2(\alpha_{11})} \int_0^1 x \ln x J_1^2(\alpha_{11} x) dx = -0.648,$$

$$\overline{\ln g} = \overline{\ln p} = \frac{1}{2\pi^2 J_1^2(\alpha_{01}) J_2^2(\alpha_{11})} \int_0^1 x dx J_0(\alpha_{01} x) J_1(\alpha_{11} x) \times \int_0^1 y dy J_0(\alpha_{01} y) J_1(\alpha_{11} y) \int_0^{2\pi} d\varphi \times \int_0^{2\pi} d\psi \cos(\varphi - \psi) \ln\left[1 - \frac{2xy}{x^2 + y^2} \cos(\varphi - \psi)\right] = -0.289,$$

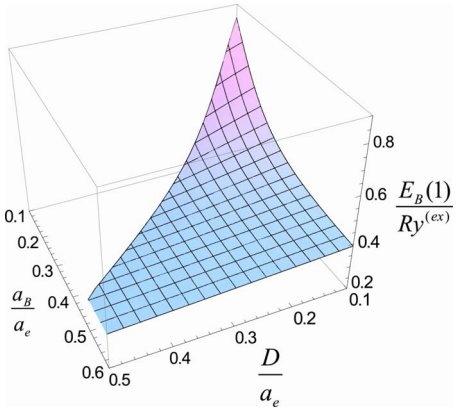

FIG. 2. (Color online) The dependence of the binding energy $E_b(1)$ scaled to the electron Rydberg constant $\mathrm{Ry}^{(e)}$ of the ground exciton state $n=1$ in the DQWR on the confinement a_B/a_e and relative width D/a_e of the insertion for the narrow barrier ($D/a_e \leq a_B/a_e$). Magnetic regime: $a_B \ll R$.

$$(g^2)_0 = \frac{8(\alpha_{01}^2 - 2)}{3\alpha_{01}^2} \frac{R^2}{a_0^2 \lambda^2}, \quad G^2 = (\alpha_{11}^2 - \alpha_{01}^2) \frac{a_0^2}{R^2},$$

$$\alpha_{01} = 2.40, \quad \alpha_{11} = 3.83,$$

and in the magnetic regime ($R \gg a_B$)

$$(\ln g)_0 = \ln \frac{2^{3/2} a_B}{a_0 \lambda} - \frac{1}{2} C, \quad (\ln g)_1 = (\ln g)_0 + \frac{1}{2},$$

$$\overline{\ln g} = \overline{\ln p} = -\frac{1}{2},$$

$$(g^2)_0 = \frac{8a_B^2}{a_0^2 \lambda^2}, \quad G^2 = \frac{2a_0^2}{a_B^2}.$$

Equations for $(\ln p)_0$ can be obtained from the corresponding equations for $(\ln g)_0$ by replacing the quantum number λ by the quantum number k. Results presented above are valid for strongly confined excitons ($r_0 \ll a_0$) subject to weak electric fields ($s\lambda^4 \ll 1$).

V. DISCUSSION

A. Indirect exciton in the double quantum wire

In the absence of an electric field the binding energy of the exciton $E_b(\lambda) = \mathrm{Ry}^{(e)}/\lambda^2$ in the DQWR containing the narrow interwire barrier ($u_0 \ll 1$, $u_0 < g$, $u_0 = 2D/a_e\lambda$) depends on the quantum number λ which in turn can be found from Eq. (27). It follows from Eq. (27) that with increasing the confinement (increasing the magnetic field, decreasing the radius of the QWR) the binding energy E_b increases. However, the wider the barrier D is, the lesser the binding energy E_b. The growth of the separation of the carriers D makes the confinement effect less pronounced. The dependence of the binding energy $E_b(\lambda)$ of the ground state $n=1$ on the confinement and on the width of the barrier D for the narrow barrier ($D/a_e \leq a_B/a_e$) is given in Fig. 2. Clearly the

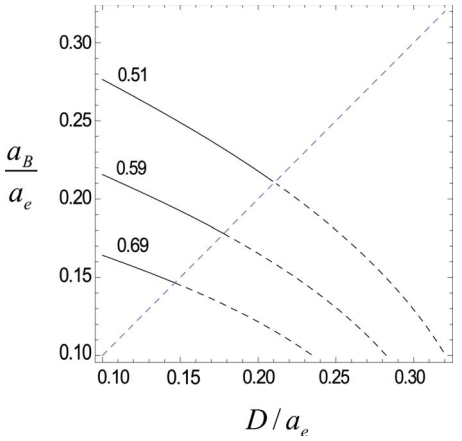

FIG. 3. (Color online) The isoenergetic contours of the binding energies $E_b(1)/\mathrm{Ry}^{(e)}=0.51$, 0.59, and 0.69 of the ground exciton state $n=1$ in the DQWR with the narrow barrier $(D/a_e \leq a_B/a_e)$, where D is the width of the insertion, a_B is the magnetic length, and a_e is the electron Bohr radius. Magnetic regime: $a_B \ll R$.

confinement and separation of the quantum wires are in competition. For special values of the magnetic field (or the radius of the QWR) and the width of the barrier, the effects of the confinement and separation of the wires cancel each other. The isoenergetic curves $E_b(1)/\mathrm{Ry}^{(e)}=\mathrm{const}$ for $D/a_e \leq a_B/a_e$ are depicted in Fig. 3.

In the limiting case of an extremely strong confinement $(g \to 0)$ and very narrow barrier $(u_0 \to 0)$, the exciton energy reads

$$E = E_g + E_\perp^{(l)} + E_n = -\frac{\mathrm{Ry}^{(e)}}{n^2} + i\frac{\Gamma_n}{2}; \quad \frac{1}{2}\Gamma_n = \frac{2\mathrm{Ry}^{(e)}}{n^3}\Delta_n,$$

where Δ_n is given by Eqs. (25) and (29).

For a finite confinement $(g \neq 0)$ and finite widths D $(u_0 \neq 0)$, the width Γ_1 of the ground exciton state $n=1$ as a function of the electric field F, and confinement (a_B/a_e) for the different insertions is presented in Fig. 4. As expected the growth of the electric field F leads to an increase in the width Γ induced by the electric field ionization of the exciton state. The stronger the confinement (the smaller the magnetic length a_B) is, the smaller the width Γ_n becomes because of an increase in the binding energy. The effect of the confinement is less pronounced with respect to that of the electric field. The reason for this is as follows: the effect of the confinement is determined by the correction δ_n to the integer n in the quantum number $\lambda = n + \delta_n$ [Eq. (27)]. In contrast to $n=0$ this correction has little effect for the states $n=1,2,\ldots$ realized in the DQWR. The broadening of the insertion further suppresses the effect of the confinement. For the ground exciton state $n=1$ in the GaAs DQWR $(\mathrm{Ry}^{(e)} \simeq 5.8$ meV, $a_e \simeq 10$ nm) with the insertion of width $D=2$ nm subject to an electric $(F=1.75$ kV/cm) and an experimentally used[1,21] magnetic field $(B=50$ T), we obtain for the width $\Gamma_1=1.45$ meV. Although the state $\lambda_0 \ll 1$ for which $\Gamma_0 < \Gamma_1$ is not realized for the indirect excitons in the DQWR, the available exciton states $n=1,2,\ldots$ in the GaAs DQWR remain stable in the presence of the electric field up to the critical value of the order of $F_0 \simeq 5.8$ kV/cm. Figures 2–4 address the magnetic field regime $a_B \ll R$. For the quantum wire regime $R \ll a_B$ the corresponding dependencies on the confinement can be found qualitatively and quantitatively with an accuracy of about 10% from those given in these figures by replacing the parameter a_B/a_0 by R/a_0.

For an intermediate barrier $(u_0 \ll 1,\ u_0 \gg g)$ the effect of the width of the interwire barrier D on the quantum number λ [Eq. (33)] becomes more pronounced and dominates that of the confinement. When the barrier width increases, the exciton binding energy $E_b(\lambda)$ decreases. As above the greater the electric field is, the wider the exciton level. The dependence of the width Γ_1 of the ground exciton state on the electric field and on the width of the barrier is shown in Fig. 5. The weak dependence of the width Γ_1 on the width of the insertion is due to the fact that the narrow interwire barrier $(u_0 \ll 1)$ has little effect on the binding energies of the exciton states $n \geq 1$. Further growth of the barrier width renders the exciton binding energy $E_b(\lambda) \sim \lambda^{-2}$ [Eq. (35)] very small.

Our results obtained for indirect excitons composed of holes positioned at the interface $z_h = -\frac{1}{2}D$ can be extended to the hole layer located at an arbitrary coordinate z_h. In this

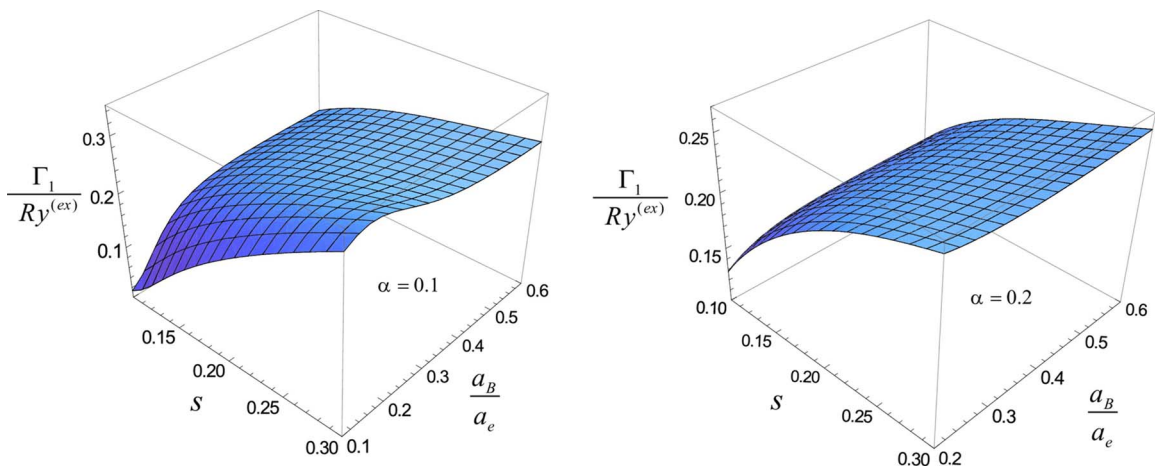

FIG. 4. (Color online) The width Γ_1 of the ground exciton state $n=1$ in the DQWR as a function of the dimensionless electric field $s = ea_eF/\mathrm{Ry}^{(e)}$ and confinement a_B/a_e for the different relative width $\alpha = D/a_e = 0.1, 0.2$ of the insertion. Magnetic regime: $a_B \ll R$.

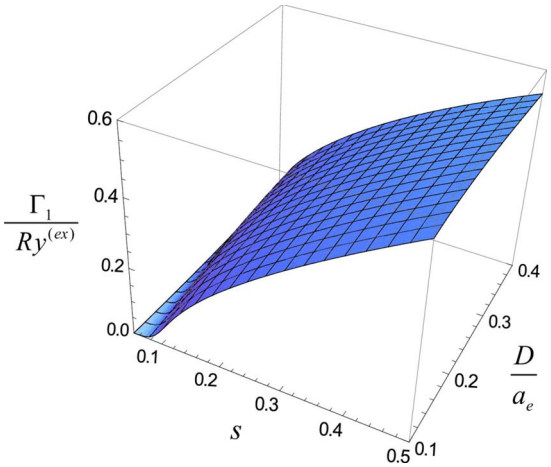

FIG. 5. (Color online) The relative width Γ_1 of the ground exciton state $n=1$ in the DQWR versus the dimensionless electric field $s=ea_eF/\mathrm{Ry}^{(e)}$ and insertion width D/a_e.

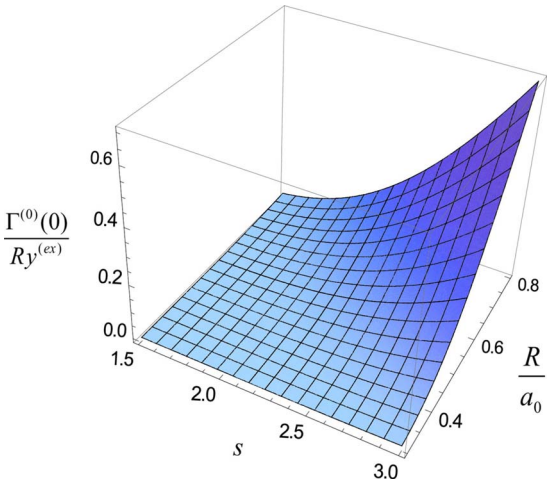

FIG. 6. (Color online) The dependence of the width $\Gamma^{(0)}(0)$ (50) of the ground exciton peak $n=0$ of the ground $l=0$ subband in the UQWR scaled to the exciton Rydberg constant $\mathrm{Ry}^{(\mathrm{ex})}$ on the dimensionless electric field $s=ea_0F/\mathrm{Ry}^{(\mathrm{ex})}$ and confinement R/a_0. Quantum wire regime: $R \ll a_B$.

case the quantum numbers $\nu(z_h,F)$ determining the exciton energy levels $-\mathrm{Ry}^{(e)}/\nu^2(z_h,F)$ can be obtained from those calculated from Eqs. (21) and (26) by replacing D by $\frac{1}{2}D - z_h$. For a broad range of semiconductors with considerably different electron and hole masses ($m_e \ll m_h$), the obtained exciton energies can be treated as the first step in the adiabatic approximation taking into account the motion of the holes. As a next step the energies E of the indirect exciton $E=E_g+E_\perp^{(l)}+E_h$ can be found from equation

$$-\frac{\hbar^2}{2m_h}\varphi^{(l)\prime\prime}(z_h)-\left(\frac{\mathrm{Ry}^{(e)}}{\nu^2(z_h,F)}+E_h\right)\varphi^{(l)}(z_h)=0,$$

with the boundary condition $\varphi^{(l)}(-\frac{1}{2}D)=0$. Numerical calculations are required.

B. Direct exciton in the uniform quantum wire

In the SS approximation we find that optical absorption (45) in the vicinity of the n exciton peak position (48) possesses a Lorentzian form (49) determined by the width $\Gamma^{(l)}(n)$ [Eq. (50)] and the shift $\Delta E^{(l)}(n)$ [Eq. (51)] both induced by the ionization of the exciton by the electric field F. The greater the confinement (the lesser the ratios a_B/a_0 and R/a_0) is, the lesser are the exciton width $\Gamma^{(l)}(n)$ [Eq. (50)] and the shift $\Delta E^{(l)}(n)$ [Eq. (51)]. With increasing electric field the width $\Gamma^{(l)}(n)$ [Eq. (50)] and shift $\Delta E^{(l)}(n)$ [Eq. (51)] both increase. The width $\Gamma^{(0)}(0)$ [Eq. (50)] of the ground exciton peak $n=0$ associated with the ground electron-hole subband $l=0$ as a function of the confinement (R/a_0) and the electric field F is provided in Fig. 6. Since the width of the ground exciton peak is proportional to $\Gamma^{(0)}(0) \sim \exp(-4/3\lambda_0^3 s)$, we need $\lambda_0^3 s \lesssim 1$ for a substantially nonvanishing $\Gamma^{(0)}(0)$. The confinement parameter $R/a_0=0.6$ provides the quantum number $\lambda_0=0.42$, which in turn leads to a significant width $\Gamma^{(0)}(0)$ for the relative electric field $s \simeq 2.5$. The isowidth curves $\Gamma^{(0)}(0)=\mathrm{const}$ are depicted in Fig. 7.

Note that the width $\Gamma^{(l)}(n)$ [Eq. (50)] and the shift $\Delta E^{(l)}(n)$ [Eq. (51)] can be calculated by the same method as that used in Sec. III. On replacing real function (41) by complex function (22) having the asymptotics of an outgoing wave, we arrive at the set (23), (24), (39), and (40). Solving this set by the determinantal method we obtain the equation for the complex quantum number λ

$$\frac{\tilde{\Phi}^2}{2}\Gamma(1-\lambda)\left[\frac{\Gamma(-\lambda)}{\zeta(\lambda)}+\frac{\cos\pi\lambda}{\Gamma(1+\lambda)}\right]+i=0, \tag{72}$$

and resulting in the complex exciton energy

$$\tilde{E}_{\mathrm{ex}}^{(l)}(n)=E_{\mathrm{ex}}^{(l)}(n)+\Delta E_{\mathrm{ex}}^{(l)}(n)-\frac{i}{2}\Gamma^{(l)}(n), \tag{73}$$

where the energy $E_{\mathrm{ex}}^{(l)}(n)$ is the discrete exciton energy level at $F=0$ [see Eq. (49)]. In this equation the width $\Gamma^{(l)}(n)$ and shift $\Delta E_{\mathrm{ex}}^{(l)}(n)$ coincide, respectively, with those in Eqs. (50) and (51) obtained from Eq. (45).

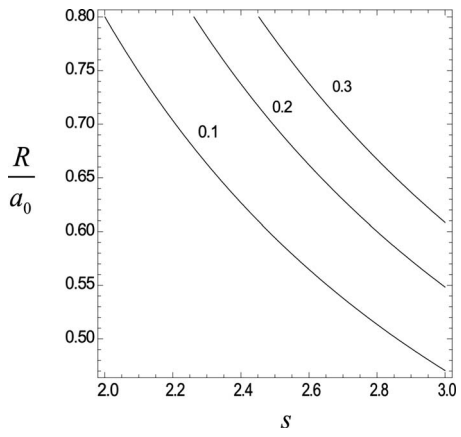

FIG. 7. The isowidth contours $\Gamma^{(0)}(0)/\mathrm{Ry}^{(\mathrm{ex})}=\alpha$ of the ground exciton peak $n=0$ of the ground $l=0$ subband in the UQWR. See Fig. 6 for units.

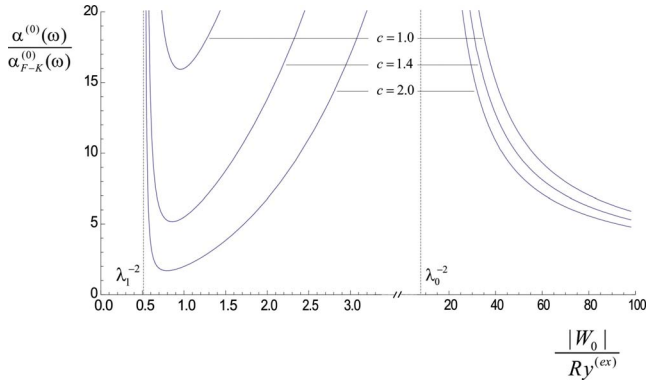

FIG. 8. (Color online) The ratio of the coefficients of the exciton $\alpha^{(0)}(\omega)$ and Franz-Keldysh $\alpha^{(0)}_{F\text{-}K}(\omega)$ electroabsorption calculated from Eq. (55) versus the red energy shift relative to the ground zero intersubband edge scaled to the exciton Rydberg constant $\mathrm{Ry}^{(\mathrm{ex})}$ for the different electric field strengths F, determined by the parameter $c=W_F/\mathrm{Ry}^{(\mathrm{ex})}$. Confinement parameter is taken to be $R/a_0=0.3$. Quantum wire regime: $R \ll a_B$.

The above mentioned complex energies of the exciton can be found by calculating the poles of the scattering matrix $S(\vartheta)$ closely related to the phase ϑ,[38]

$$S(\vartheta)=\exp[2i\vartheta]=\frac{\cot\vartheta+i}{\cot\vartheta-i}. \tag{74}$$

Equating the denominator to zero and using Eq. (44) for $\cot\vartheta$, we immediately arrive at Eq. (72) and to the corresponding complex energy levels.

The exciton effect induces not only a quasi-Rydberg series of the maxima of absorption but for the frequencies distant from the positions of the exciton peaks, the exciton attraction modifies strongly the optical absorption. The ratio $\alpha^{(0)}(\omega)/\alpha^{(0)}_{F\text{-}K}$ [Eq. (55)] versus the energy deviation $W_0<0$ from the ground threshold $\hbar\omega^{(0)}=E_g+E^{(0)}_{\perp}(W_0=0)$ is presented in Fig. 8. As expected the exciton effect has a maximum in the vicinity of the exciton peak positions determined by the ground $\lambda_0=0.35$ and first-excited $\lambda_1=1.39$ quantum numbers calculated from Eq. (47) at $\beta=R/a_0=0.3$, and then rapidly decreases reaching a minimum at intermediate frequencies. As the frequency moves away from the main exciton peak toward the gap $|W_0/\mathrm{Ry}^{(\mathrm{ex})}|>\lambda_0^{-2}$, the influence of the electron-hole attraction gradually decreases. The greater the electric field is, the lesser the effect of the exciton on the F-K electroabsorption. Note that for laboratory electric fields the exciton mechanism of absorption dominates that of the photon-assisted tunneling (F-K effect). For the electric field providing the condition $W_F=\mathrm{Ry}^{(\mathrm{ex})}$, the minimum exciton effect takes place at the frequency shift $|W_0|\simeq\mathrm{Ry}^{(\mathrm{ex})}$. In this case the exciton absorption $\alpha^{(0)}$ exceeds the F-K electroabsorption $\alpha^{(0)}_{F\text{-}K}$ by a factor of 16. The same ratio is valid for the frequency shift $|W_0|\simeq 35\mathrm{Ry}^{(\mathrm{ex})}$ in the region below the ground exciton peak λ_0. This factor overcomes that corresponding to the bulk material[28] because the binding energy of the quasi-1D exciton $\mathrm{Ry}^{(\mathrm{ex})}/\lambda_0^2$ overcomes that of the exciton in bulk crystal $\mathrm{Ry}^{(\mathrm{ex})}$. For the magnetic regime ($a_B/a_0=0.3$) the corresponding results can be obtained from Fig. 8 with an accuracy of about 10% by replacing R by a_B. With increasing the confinement (decreasing the parameters R and a_B) the peak positions $\sim\lambda_{0,1}^{-2}$ in Fig. 8 are displaced toward greater values $|W_0|/\mathrm{Ry}^{(\mathrm{ex})}$. Although the absorption coefficients $\alpha^{(l)}(\omega)$ and $\alpha_{F\text{-}K}(\omega)$ depend on the confinement $\sim r_0^{-2}$, its dimensionless ratio [Eq. (55)] does not depend on the radius of the QWR and on the strong magnetic field.

At this stage it is appropriate to apply the results obtained in Sec. IV B to the description of the continuous exciton absorption above the threshold $\hbar\omega>E_g+E^{(l)}_{\perp}$. Matching the wave function $\psi^{(0)}(v)$ [Eq. (61)] and the wave function $\psi^{(0)}(v)$ decreasing at $v\to-\infty$, and obtained from Eq. (41) by replacing λ by k, we arrive at Eq. (64) for $\vartheta=\frac{\pi}{2}$. The latter equation being united with Eq. (62) leads to the coefficient of the optical absorption $\alpha^{(l)}(\omega)=\beta_0^2/r_0^2$ in the form

$$\alpha^{(l)}(\omega)=\frac{2\mu a_0}{\pi\hbar^2 r_0^2}Z(k)k\sin^2\left[\frac{2\mathrm{Ry}^{(\mathrm{ex})}}{3ea_0Fk^3}-k\ln\frac{8\mathrm{Ry}^{(\mathrm{ex})}}{ea_0Fk^3}-\frac{\pi}{4}+\sigma(k)\right],$$

$$\text{where } k=\left(\frac{\mathrm{Ry}^{(\mathrm{ex})}}{\hbar\omega-E_g-E^{(l)}_{\perp}}\right)^{1/2}. \tag{75}$$

The above equation describes the F-K effect, i.e., frequency oscillations modulated by the reciprocal square-root factor, which in turn are modified by the Sommerfeld factor relevant to the 1D exciton

$$Z(k)=\frac{\sinh\pi k}{\pi k}e^{-\pi k}.$$

In the region distant from the threshold [$k\ll 1$ $Z(k)\simeq 1$], these oscillations are the same as those calculated numerically[2,15,16] and observed experimentally.[45] Our results are in line with those obtained for the exciton absorption in bulk semiconductors.[28,29] The equation for the wave function ψ describing the exciton with an energy corresponding to the threshold of absorption can be obtained from Eq. (58) neglecting the off-diagonal term and setting $k=0$

$$\psi''(w)+p(w)\psi(w)=0,$$

$$p(w)=w+\frac{2\nu}{|w|},\quad w=\left(\frac{2\mu eF}{\hbar^2}\right)^{1/3}z,\quad \nu^2=\frac{\mathrm{Ry}^{(ex)}}{W_F}.$$

Method of a comparison equation[36] gives for the wave function

$$\psi(w)=K(\varphi')^{-1/2}Ai(-\varphi),\quad K^2=\frac{4\pi\mu}{2\pi\hbar^2}\left(\frac{\hbar^2}{2\mu eF}\right)^{1/3},$$

$$\varphi(w)=\left[\frac{3}{2}\Theta(w)\right]^{2/3},$$

$$\Theta(w)=\int_{-\sqrt{2\nu}}^{w}p^{1/2}(v)dv,$$

which in turn leads to the coefficient of the optical absorption $\alpha^{(l)}(\omega_0)=|\psi(0)|^2/r_0^2$ at the edge $\hbar\omega_0=E_g+E^{(l)}_{\perp}$

$$\alpha^{(l)}(\omega_0) = \alpha_{F\text{-}K}(\omega_0)(1 + b\nu), \quad \alpha_{F\text{-}K}(\omega_0) = \frac{K^2}{r_0^2 3^{4/3}\Gamma^2(2/3)},$$

$$b = \frac{3^{1/3}2^{4/3}\pi^{1/2}\Gamma(5/6)}{\Gamma^{4/3}(3/4)}, \quad \nu \ll 1. \tag{76}$$

As above, the exciton attraction ($\nu \neq 0$) increases the F-K optical absorption in the vicinity of the edge. The enhancement of the electroabsorption at the edge induced by the excitonic effect has been calculated numerically in Refs. 15 and 16. The obtained analytical equations describe completely the optical absorption both below the threshold close to the exciton peaks [Eq. (49)] and between them [Eq. (55)], as well as above the threshold at the edge [Eq. (76)] and distant from the edge [Eq. (75)]. In summary, below the threshold the optical spectrum is formed by the quasi-Coulomb series of the exciton peaks of finite width, on which the tail of F-K absorption, exponentially decreasing toward the low frequencies, is imposed. These peaks condense in the vicinity of the threshold, providing the finite absorption. Above the threshold the F-K oscillations of the decreasing amplitude are found to occur.

With increasing the electric field $F \sim s$ the exciton peaks become wider [$\Gamma^{(l)}(n) \sim \tilde{\Phi}^2$] and less in intensity ($\alpha^l_{\max} \sim \tilde{\Phi}^{-2}$) with $\tilde{\Phi}^2 \sim \exp(-4/3n^3 s)$. The greater the confinement, i.e., the greater the magnetic field B and the lesser the radius of the quantum wire R, the lesser is the width of the exciton peak $\Gamma^{(l)}(n)$ and the greater the binding energy $E_b^{(l)}(n)$ of the corresponding exciton state and the intensity of the exciton peak $\alpha^l_{\max} \sim r_0^{-2}$, where $r_0 \sim B^{-1/2}, R$. In spite of the growth of the binding energy [$E_b^{(l)}(0) \sim \ln^2 r_0/a_0$] the peak position $\hbar\omega = E_g + E_\perp^{(l)} - E_b^{(l)}(n)$ is shifted to higher frequencies because the blueshift induced by the transverse energies $E_\perp^{(l)} \sim R^{-2}, B$ exceeds the redshift associated with the binding energy $E_b^{(l)}(n)$. In the regions between the exciton peaks the electroabsorption increases with increasing both the electric field and confinement with $\alpha^{(l)}(\omega) \sim r_0^{-2}$. In the region above the effective band gap $E_g + E_\perp^{(l)}$ electroabsorption manifests itself via frequency oscillations modulated by the reciprocal root factor $\sim(\hbar\omega - E_g - E_\perp^{(l)})^{-1/2}$. With increasing electric field F the period of the frequency oscillations $\Delta\omega$ is widened as $\Delta\omega \sim F^{2/3}$. The greater the confinement the greater is the absorption $\alpha^{(l)}(\omega) \sim r_0^{-2}$. At the threshold $\hbar\omega = E_g + E_\perp^{(l)}$ the coefficient of absorption $\alpha^{(l)}(\omega)$ decreases with increasing electric field according to $F^{-1/3}$ and increases with increasing confinement $\sim r_0^{-2}$.

In the DS 0–1 approximation Eqs. (66) and (67) describe the interplay between the electric field ionization and intersubband autoionization reflected in the exciton absorption. Since the electric field ionization has been discussed above, below we briefly focus on the effect of autoionization. In the vicinity of the resonances the absorption has Lorentzian forms (48), (49), and (69). In the logarithmic approximation $|g \ln g| \ll 1$, $|p \ln p| \ll 1$, $k \simeq G^{-1}$, $\sin\gamma_0 \simeq 1$, $\cos\gamma_0 \sim G^{-1}$, $\eta_0(k) \sim$ const for the ground exciton state $n=0$, Eqs. (70) and (71) provide for the resonant width $\Gamma(0)$ and shift $\Delta E(0)$, respectively,

$$\Gamma(0) \simeq 2^{5/2}\frac{a_B}{a_0}\left|\ln\frac{a_B}{a_0}\right|\mathrm{Ry}^{\mathrm{ex}}; \quad \Delta E(0) = -\frac{\gamma_E + 2\ln 2}{2^{3/2}}\frac{a_B}{a_0}\Gamma(0),$$

for the magnetic regime $a_B \ll R \ll a_0$, and

$$\Gamma(0) \simeq \frac{32\overline{\ln g^2}}{\sqrt{\alpha_{11}^2 - \alpha_{01}^2}}\frac{R}{a_0}\left|\ln\frac{R}{a_0}\right|\mathrm{Ry}^{\mathrm{ex}};$$

$$\Delta E(0) = -\frac{\gamma_E + \frac{1}{2}\ln(\alpha_{11}^2 - \alpha_{01}^2)}{\sqrt{\alpha_{11}^2 - \alpha_{01}^2}}\frac{R}{a_0}\Gamma(0),$$

for the quantum wire regime $R \ll a_B \ll a_0$.

It is clear that the confinement destroys the intersubband coupling that in turn leads to the fact that the resonance width and shift decrease. Neglecting the coupling ($a_B/a_0 \to 0$, $R/a_0 \to 0$) we obtain from Eqs. (48) and (49) the δ function-type peaks $\alpha^{(l)}(\omega, n) = \alpha_0(n)\delta[\hbar\omega - E_{\mathrm{ex}}^{(l)}(n)]$, corresponding to optical transitions to the strictly discrete exciton peaks. Note that our results obtained for the intersubband couplings (48), (49), and (69)–(71) correlate completely with those derived from Fano theory,[25] which takes into account the interference of degenerate discrete and continuum states. Following this theory the density of the exciton states in the vicinity of the maxima possesses a Lorentzian profile [the same as that given by Eq. (49)] in which the resonant width $\Gamma(n)$ and shift $\Delta E(n)$ depend on the matrix element of the off-diagonal potential $V_0^1(z)$ calculated with respect to the functions of the degenerate discrete and continuum states. Taking Eq. (17) at $B=0$ and Eq. (61) at $\Lambda=0$ for the discrete $\psi(u)$ and continuous $\psi(v)$ states, respectively, we immediately calculate the width $\Gamma(n) = 2\pi|\langle\psi(u)|V_0^1(z)|\psi^0(v)\rangle|^2$ coinciding with Eq. (70).

On replacing real function (61) by the complex function $\psi^{(0)}(v) \sim W_{is,1/2}(-iv)$ possessing the asymptotics of an the outgoing wave and matching this function with that obtained by the double integration of Eq. (58), we find the equation for the complex quantum number λ

$$\psi(1 - ik) + \frac{1}{2ik} + 2\gamma_E - i\frac{\pi}{2} + \left(\ln\frac{p}{2}\right)_0 - \frac{\overline{\ln g}\,\overline{\ln p}}{\zeta_1(\lambda)} = 0.$$

The corresponding exciton complex energy acquires form (73) in which the width $\Gamma^{(l)}(n)$ and shift $\Delta E^{(l)}(n)$ coincide, respectively, with those in Eqs. (70) and (71) obtained from Eq. (68). The same energy can be found by calculating the poles of the scattering matrix $S(Q)$ [Eq. (74)] taking cot Q from Eq. (65) for $\tilde{\Phi}=0$. The identity of the final equations for the resonant energy shift and width associated with the electric field ionization and autoionization obtained by the different techniques in frame of the Fano theory,[25] the scattering matrix method,[38] and the present approach has been discussed and justified in Refs. 43 and 44.

The combined effect of the electric field F and the intersubband coupling on the width of the ground exciton state $n=0$ is shown in Fig. 9 for the magnetic regime ($a_B \ll R$). Since the width $\Gamma(0)$ exceeds the sum $\Sigma(0)$ of the widths associated with the independent phenomena, the interplay of the autoionization and electric field-ionization processes is

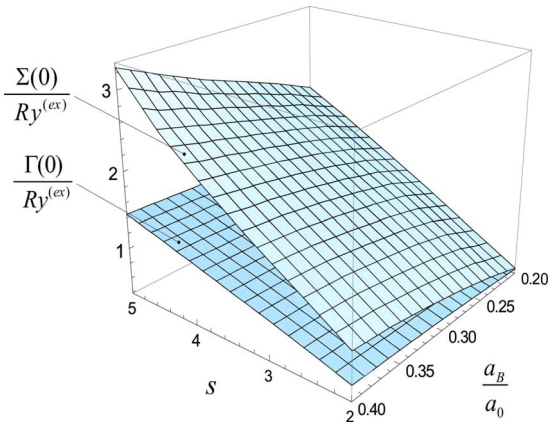

FIG. 9. (Color online) The dependence of the relative width $\Gamma(0)/\mathrm{Ry}^{(\mathrm{ex})}$ of the ground exciton resonance state $n=0$ caused by both the autoionization and the electric field ionization on the dimensionless electric field $s=ea_0F/\mathrm{Ry}^{(\mathrm{ex})}$ and confinement parameter a_B/a_0 ($\mathrm{Ry}^{(\mathrm{ex})}$ is the exciton Rydberg constant). The width $\Gamma(0)$ is calculated from Eqs. (66) and (67). The width $\Sigma(0)=\Gamma_g(0)+\Gamma_F(0)$ is the sum of the widths induced by the autoionization $[\Gamma_g(0)]$ and electric field $[\Gamma_F(0)]$ ionization calculated from Eqs. (68) and (45) for $l=1$, respectively. Magnetic regime: $a_B \ll R$.

found to occur. As expected both widths $\Gamma(0)$ and $\Sigma(0)$ and its difference increase with increasing the electric field and decreasing the confinement (decreasing the magnetic field). The effect of the electric field is governed by exponential factor (25) while that of the confinement by the logarithmic term in Eq. (46). As a result the dependence of the electric field is more pronounced compared to that on confinement. Note that for the chosen range of the parameters the combined width $\Gamma(0)$ remains less than the exciton binding energy $E_b=\mathrm{Ry}^{(\mathrm{ex})}/\lambda_0^2$. In the worst case $a_B/a_0=0.4(\lambda_0^2=0.30)$, $s=5$ we obtain $\Gamma(0)/E_b=0.42$. The results presented in Fig. 9 can be extended to the quantum wire regime ($a_B \to R$) with an accuracy of about 10%. Thus not only the strictly discrete exciton states but the exciton Fano resonances subject to the electric fields can be investigated in experiments.

Our results correlate completely with those obtained numerically. The growth of the exciton binding energy $E_b=\mathrm{Ry}^{(\mathrm{ex})}/\lambda^2$ calculated from Eqs. (46) and (47) for the quantum number λ with increasing confinement is found to occur. This is in agreement with the data obtained by the variational method,[17–20,46,47] using the model 1D quasi-Coulomb potential[48] and the semiconductor Bloch equation.[31] For the relative QWR radius $R/a_0=0.3$ the scaled binding energy is about equal to $E_b/\mathrm{Ry}^{(\mathrm{ex})} \simeq 5.6-6.0$,[2,17,46–48] while for $R/a_0=0.2$ the result $E_b/\mathrm{Ry}^{(\mathrm{ex})} \simeq 8.0$ can be extracted from Refs. 17, 46, and 48. The latter could be treated as close to the ratio $E_b/\mathrm{Ry}^{(\mathrm{ex})} \simeq 10.4$ found for $R/a_0=0.2$ from Eqs. (46) and (47) having the accuracy of the order $O(g)$ ($g \sim R/a_0, a_B/a_0$), i.e., 20% in this case. In order to avoid the cumbersome mathematics and to make the obtained analytical results transparent, we limit ourselves to the terms of the order of $\sim u$ and exponential terms $\sim \exp(\pm\frac{2}{3}|\xi|^{3/2})$ in expansions of the Whittaker functions $W_{\lambda,1/2}(u)$ and $M_{\lambda,1/2}(u)$, and the Airy functions $Ai(\xi)$ and $Bi(\xi)$ in Eqs. (17) and (22), respectively. Only terms $\sim \ln g$ are kept in the solution to Eq. (15), obtained by the iteration procedure. Taking into account terms of higher orders with respect to the expansions of the listed functions,[37] the precision of the presented analytical calculations can be essentially increased.

It follows from Eq. (50) that the width of the exciton peak $\Gamma^{(l)}(n)$ increases with increasing electric field strength and decreasing confinement. The growth of the width of the exciton maximum with the growth of the electric field and with the reduction in the magnetic field has been demonstrated clearly.[31] The width of the exciton peak $\Gamma^{(0)}(0)=7.2$ meV [Eq. (50)] and that given in Ref. 2 $\Gamma^{(0)}(0) \simeq 6.5$ meV for a GaAs QWR ($\mathrm{Ry}^{(\mathrm{ex})}=4.2$ meV, $a_0=14$ nm) of radius 4.2 nm ($E_b=23.6$ meV, $\lambda_0=0.42$) exposed to an electric field $F=15$ kV/cm ($s=5$) do agree quite well. The T-shaped form of the QWR considered in Ref. 31 prevents us a direct comparison of our result to those of Ref. 31.

As mentioned above the presented analytical results have been obtained for narrow QWRs ($R/a_0 \ll 1$) and/or in the presence of strong magnetic ($a_B/a_0 \ll 1$) and weak electric ($s\lambda^4 \ll 1$) fields. We assumed that the electron and hole in the indirect exciton were separated by a narrow insertion ($D/a_0 \ll 1$), and its motion of the carriers is bound by impenetrable barriers of heights V_j, $j=e,h$. The latter implies that the size-quantized level $E_{\perp l_j}$ [Eq. (10)] is positioned far away from the top of the barrier V_j, i.e., ($R \gg R_{0j}$), where $R_{0j}=(\hbar^2\alpha^2/2m_jV_j)^{1/2}$, $\alpha=2.40$. In spite of the number of approximations made, most of them correspond to those employed in recent theoretical and experimental studies. The cylindrical InGaAs/InP QWRs ($a_0=16$ nm) of radius $R=2.5,3.6,4.5$ nm ($R/a_0=0.16,0.22,0.28$) and GaAs/AlGaAs QWR ($a_0=14$ nm) of radius $R=4.2$ nm ($R/a_0=0.30$) were under investigation in Refs. 2 and 4, respectively. Madureira *et al.*[31] considered the T-shaped GaAs QWR with the arm and step quantum wells of width $R=5.6$ nm ($R/a_0=0.40$) and $R=5.1$ nm ($R/a_0=0.36$), respectively. Maes *et al.*[21] studied the rectangular InAs/InP QWR ($a_0=35$ nm) of width $R=18$ nm ($R/a_0=0.51$) and height $R=2$ nm ($R/a_0=0.057$). Magnetic fields up to the values $B=50$ T ($a_B/a_0=0.10$) were applied to the excitons in the InAs QWRs.[1,3,21] The effect of the electric fields up to the maximum strength $F=15$ kV/cm ($s=5$) and $F=6$ kV/cm ($s=2$) on the exciton states in the GaAs QWRs have been studied in Refs. 2 and 31. The quantum number $\lambda_0=(\mathrm{Ry}^{(\mathrm{ex})}/E_b)^{1/2}$ for the ground state was estimated from the binding energies $E_b=23.6$ meV (Ref. 2) and $E_b=9.0$ meV,[31] and the exciton Rydberg constant $\mathrm{Ry}^{(\mathrm{ex})}=4.2$ meV to give the results $\lambda_0=0.42$ and $\lambda_0=0.68$, respectively. Thus we have for the parameter $s\lambda_0^4$ the maximal values 0.16 and 0.42 for the excitons referred to Refs. 2 and 31, respectively. The critical electric field F_0, providing the complete ionization of the ground exciton state, estimated from the condition $s\lambda_0^3 \simeq 1$, is found to be $F_0^{(\mathrm{bulk})} \simeq 3$ kV/cm for the bulk GaAs material ($\lambda_0=1$) and $F_0^{(\mathrm{qwr})} \simeq 40.5$ kV/cm for the GaAs QWR ($\lambda_0=0.42$) investigated in Ref. 2. The InP insertions of width ($D=4$ and 7 nm) in the InGaAs [$a_0=16$ nm($D/a_0=0.25$)] (Ref. 4) and InAs [$a_0=35$ nm ($D/a_0=0.20$)] (Ref. 9) QWRs have been incorporated, respectively.

Above we have avoided to deal with QWRs possessing an extremely small radius. We note that narrowing the QWR providing the lateral confinement ($R \ll a_0$) is in conflict with the infinite barrier approximation $R \gg R_{0j}$. In order to satisfy both of these conditions, extended exciton states in the QWRs with considerable band offsets should be taken. Thus, the GaAs/$Al_{0.3}Ga_{0.7}$As QWR of radius $R=4.2$ nm for which $a_0=14$ nm, $m_e=0.067m_0$, $V_e=225$ meV,[49] and $(R_{0e}/R)^2 \simeq 0.72$, is not the best candidate to be described by the infinite barrier approximation while the InAs/InP QWR of radius $R=8.0$ nm having the parameters $a_0=35$ nm, $m_e=0.023m_0$, and $V_e=657$ meV (Ref. 50) is more suitable for this approximation because of the ratio $(R_{0e}/R)^2 \simeq 0.20$. For the QWRs of smaller radius the penetration of the electron and hole states into the barrier material should be taken into account.[21]

In the case of anisotropic energy bands[3] with the effective masses $m_{\parallel,\perp j}$ $(j=e,h)$ corresponding to the motion parallel and perpendicular to the QWR z axis, respectively, the exciton states depend on the ratio $m_{\perp j}/m_{\parallel j}$ that in principle requires a numerical study. However, in a narrow QWR ($R \ll a_0$) the transverse size-quantized states are determined by the effective mass $m_{\perp j}$ while the longitudinal motion is governed by the Coulomb potential and the effective mass $m_{\parallel j}$. This allows obtaining of the final results for the exciton binding energy, the exciton peak position, and the resonance shifts and widths by replacing in Eqs. (10) and (13) m_j by $m_{\perp j}$ and further $\mathrm{Ry}^{(e)}$ by $\mathrm{Ry}^{(e)}\frac{m_{\parallel e}}{m_e}$, a_e by $a_e\frac{m_e}{m_{\parallel e}}$, $\mathrm{Ry}^{(\mathrm{ex})}$ by $\mathrm{Ry}^{(\mathrm{ex})}\frac{\mu_\parallel}{\mu}$, and a_0 by $a_0\frac{\mu}{\mu_\parallel}$ where $\mu_{\parallel,\perp}^{-1}=\mu_{\parallel,\perp e}^{-1}+\mu_{\parallel,\perp,h}^{-1}$.

Along with the barriers of finite height the image charges caused by the difference between the dielectric constants of the wire ε_w and barrier ε_b materials influence the exciton states. The effect of the dielectric-constant mismatch has been studied by Bányai *et al.*[48] using the model 1D quasi-Coulomb potential. For the ratio $\varepsilon_w/\varepsilon_b=1.3$ the contribution of the dielectric-constant mismatch to the relative exciton binding energy $E_b/\mathrm{Ry}^{(\mathrm{ex})}$ at $R/a_0=0.5$ is about 17%. This value is comparable to the correction of the order of 12.5% caused by the finite barrier bound the GaAs/$Al_{0.3}Ga_{0.7}$As QWR of the same radius.[17]

For the QWRs of intermediate thickness or those subject to moderate magnetic fields for which the radius of the QWR and/or the magnetic length are comparable to the exciton Bohr radius, the single- and double-subband approximation become less appropriate. In this case the spectrum of the exciton absorption can be obtained via the multisubband approximation. Only at the final stage of the determinantal procedure some numerical calculations are necessary. We expect that in the multisubband approximation series (3) and (36) are rapidly convergent similar to those describing the diamagnetic resonant states.[51] It was found that the multisubband approximation[51] does not lead to significant qualitative changes relative to the double-subband model employed here

In order to estimate the values to be expected in an experiment, we take for the GaAs QWR the parameters for the electron (exciton) Rydberg constant $\mathrm{Ry}^{(e)}=5.8$ meV ($\mathrm{Ry}^{(\mathrm{ex})}=4.2$ meV) and for the electron (exciton) Bohr radius $a_e=9.8$ nm ($a_0=14$ nm). In the presence of a magnetic field $B=32$ T the narrow insertion of width $D=2.0$ nm reduces the binding energy $E_b(1)$ of the ground state of the indirect exciton up to the value $E_b(1)=2.2$ meV. The same magnetic and electric fields $F=1.6$ kV/cm applied to the DQWR with the same insertion render the ground state of the indirect exciton sufficiently stable with the width $\Gamma_1=1.4$ meV and lifetime $\tau_1=\hbar/\Gamma_1=0.45$ ps. The width of the indirect exciton state Γ_1 in the DQWR of radius $R \lesssim 3$ nm containing the insertion of the intermediate width $D=3.9$ nm and subject to the same electric field F is equal to about $\Gamma_1=2.2$ meV. For the direct excitons in the QWR of radius $R=5.6$ nm the width of the ground state associated with the ground subband $\Gamma^{(0)}(0)$ caused by electric field $F=12$ kV/cm ionization is of the order of $\Gamma^{(0)}(0)=1.0$ meV. The period of the first Franz-Keldysh oscillations is $\hbar\Delta\omega \simeq 16$ meV, which is very close to the period, calculated by Hughes and Citrin.[16] For the effective band gap we have $\hbar\omega^{(0)}=E_g+E_\perp^{(0)} \simeq 1.65$ eV. The chosen electric fields on the one hand allow the excitons to be confined and sufficiently stable within the QWRs, and on the other hand provide a substantially nonvanishing width of the energy levels, which can be measured experimentally. We believe that the presented analytical approach being together with the numerical results provides a further development of our understanding of magnetoexcitons in biased QWRs.

VI. CONCLUSION

In summary, we have developed an analytical approach to the problem of the exciton in a thin uniform and double QWRs exposed to the electric and strong magnetic fields that are both directed parallel to the QWR axis. The radius of the QWR and the underlying magnetic length are taken to be much less than the exciton Bohr radius providing a strong confinement and quasi-1D character of the exciton states. The dependencies of the complex energy levels of the indirect excitons in the double QWR on the QWR radius, and magnetic and electric field strengths and width of the insertion embedded in the double QWR were derived. The exciton binding energy increases with increasing confinement and decreasing width of the interwire insertion. The stronger the electric field is, the larger becomes the width of the exciton level. The broadening decreases with increasing exciton binding energy. The coefficient of the exciton absorption in the uniform QWRs as a function of the confinement parameters (R,a_B) and electric field strength has been calculated explicitly. The effect of the electric field on the width of the exciton peaks is qualitatively the same as that on the width of the quasidiscrete exciton levels in the double QWR. In the spectral region away from the positions of the exciton peak, the exciton effect considerably increases the *F-K* electroabsorption associated with the photon-assisted interband tunneling. The coefficient of absorption taking into account the exciton ionization through the two channels, namely, the electric field ionization and autoionization caused by the intersubband coupling, is analytically derived within the two-subband approximation. The approximations employed in this work correspond to the parameters of the QWRs and external fields chosen for the experimental and theoretical

studies. Our analytical results correlate well with those calculated numerically. Estimates of the expected experimental values made for the parameters of a GaAs/AlGaAs QWR show that the effects of the exciton confinement, induced by the barrier material and magnetic field, as well as electric field ionization and autoionization, can be observed experimentally.

ACKNOWLEDGMENT

The authors are grateful to V. Bezchastnov and D. Turchinovich for valuable discussions, and to C. Morfonios for his assistance with respect to technical aspects of this work. B.S.M. thanks the Deutsche Forschungsgemeinschaft for financial support.

[1] Y. Sidor, B. Partoens, F. M. Peeters, J. Maes, M. Hayne, D. Fuster, Y. Gonzalez, L. Gonzalez, and V. V. Moshchalkov, Phys. Rev. B **76**, 195320 (2007).
[2] T. Y. Zhang and W. Zhao, Phys. Rev. B **73**, 245337 (2006).
[3] Y. Sidor, B. Partoens, and F. M. Peeters, Phys. Rev. B **71**, 165323 (2005).
[4] T. Y. Zhang, W. Zhao, J. C. Cao, and G. Qasim, J. Appl. Phys. **98**, 094311 (2005).
[5] K. Yamamoto, T. Kamata, S. Iwai, S. Kazaoui, N. Minami, F. Mizukami, K. Misawa, T. Ohta, and T. Kobayashi, Chem. Phys. Lett. **302**, 609 (1999).
[6] S. P. McGinnis, B. Das, and M. Dobrowolska, Thin Solid Films **365**, 1 (2000).
[7] S. Gradečak, F. Qian, Y. Li, H.-G. Park, and C. M. Lieber, Appl. Phys. Lett. **87**, 173111 (2005).
[8] M. Tchernycheva, G. E. Cirlin, G. Patriarche, L. Travers, V. Zwiller, U. Perinetti, and J.-C. Harmand, Nano Lett. **7**, 1500 (2007).
[9] M. T. Björk, B. J. Ohlsson, C. Thelander, A. I. Persson, K. Deppert, L. R. Wallenberg, and L. Samuelson, Appl. Phys. Lett. **81**, 4458 (2002).
[10] M. Zervos and L.-F. Feiner, J. Appl. Phys. **95**, 281 (2004).
[11] W. Franz, Z. Naturforsch. A **13**, 484 (1958).
[12] L. V. Keldysh, Sov. Phys. JETP **34**, 788 (1958).
[13] N. Haug and S. W. Koch, *Quantum Theory of the Optical and Electronic Properties of Semiconductors*, 4th ed. (World Scientific, New Jersey, 2005).
[14] P. Y. Yu and M. Cardona, *Fundamentals of Semiconductors. Physics and Material Properties*, 3rd ed. (Springer, Berlin, 2001).
[15] T. G. Pedersen and T. B. Lynge, Phys. Rev. B **65**, 085201 (2002).
[16] S. Hughes and D. S. Citrin, Phys. Rev. Lett. **84**, 4228 (2000).
[17] G. Li, S. V. Branis, and K. K. Bajaj, J. Appl. Phys. **77**, 1097 (1995).
[18] A. Balandin and S. Bandyopadhyay, Phys. Rev. B **52**, 8312 (1995); Superlattices Microstruct. **19**, 97 (1996).
[19] P. Villamil, C. Beltran, and N. Porras-Montenegro, J. Phys.: Condens. Matter **13**, 4143 (2001).
[20] E. Kasapoglu, H. Sari, and I. Soekmen, Surf. Rev. Lett. **10**, 737 (2003).
[21] J. Maes, M. Hayne, Y. Sidor, B. Partoens, F. M. Peeters, Y. González, L. González, D. Fuster, J. M. Garcia, and V. V. Moshchalkov, Phys. Rev. B **70**, 155311 (2004).
[22] Yu. Lozovik and A. M. Ruvinskii, J. Exp. Theor. Phys. **85**, 979 (1997).
[23] A. S. Arkhipov, G. E. Astrakharchik, A. V. Belikov, and Yu. E. Lozovik, JETP Lett. **82**, 39 (2005).
[24] V. V. Krivolapchuk, A. L. Zhmodikov, and E. S. Moskalenko, Phys. Solid State **48**, 150 (2006).
[25] U. Fano, Phys. Rev. **124**, 1866 (1961).
[26] T. Yamabe, A. Tachibana, and H. J. Silverstone, Phys. Rev. A **16**, 877 (1977).
[27] S. Bednarek, B. Szafran, T. Chwiej, and J. Adamowski, Phys. Rev. B **68**, 045328 (2003).
[28] I. A. Merkulov and V. I. Perel', Phys. Lett. **45**, 83 (1973).
[29] A. G. Aronov and A. S. Ioselevich, Sov. Phys. JETP **47**, 548 (1978).
[30] S. Benner and H. Haug, Phys. Rev. B **47**, 15750 (1993).
[31] J. R. Madureira, M. Z. Maialle, and M. H. Degani, Phys. Rev. B **66**, 075332 (2002).
[32] W. Lamb, Phys. Rev. **85**, 259 (1952).
[33] L. P. Gor'kov and I. E. Dzyaloshinskii, Sov. Phys. JETP **26**, 449 (1968).
[34] A. G. Zhilich, J. Halpern, and B. P. Zakharchenya, Phys. Rev. **188**, 1294 (1969).
[35] H. Hasegawa and R. E. Howard, J. Phys. Chem. Solids **21**, 179 (1961).
[36] S. Yu. Slavyanov, *Asymptotic Solution to the One-dimensional Schrödinger Equation* (American Mathematical Society, Philadelphia, PA, 1996).
[37] *Handbook of Mathematical Functions*, edited by M. Abramowitz and I. A. Stegun (Dover, New York, 1972).
[38] R. G. Newton, *Scattering Theory of Waves and Particles*, 2nd ed. (Springer, New York, 1982).
[39] B. S. Monozon and A. G. Zhilich, Sov. Phys. JETP **73**, 1066 (1991).
[40] R. J. Elliott, Phys. Rev. **108**, 1384 (1957).
[41] B. S. Monozon and M. V. Pevzner, Sov. Phys. Semicond. **4**, 390 (1970).
[42] A. G. Zhilich and O. A. Maksimov, Sov. Phys. Semicond. **9**, 616 (1975).
[43] B. S. Monozon and P. Schmelcher, Phys. Rev. B **71**, 085302 (2005).
[44] B. S. Monozon and P. Schmelcher, Phys. Rev. B **75**, 245207 (2007).
[45] A. Horvath, G. Weiser, C. Lapersonne-Meyer, M. Schott, and S. Spagnoli, Phys. Rev. B **53**, 13507 (1996).
[46] M. H. Degani and O. Hipólito, Phys. Rev. B **35**, 9345 (1987).
[47] J. W. Brown and H. N. Spector, Phys. Rev. B **35**, 3009 (1987).
[48] L. Bányai, I. Galbraith, C. Ell, and H. Haug, Phys. Rev. B **36**, 6099 (1987).
[49] G. Creci and G. Weber, Semicond. Sci. Technol. **14**, 690 (1999).
[50] I. Vurgaftman, J. R. Meyer, and L. R. Ram-Mohan, J. Appl. Phys. **89**, 5815 (2001).
[51] A. G. Zhilich and B. K. Kyuner, Sov. Phys. Semicond. **15**, 1108 (1981).